THE JOURNAL OF COMPARATIVE NEUROLOGY 233:48-90 (1985)

Tectoreticular Pathways in the Turtle, *Pseudemys scripta*. I. Morphology of Tectoreticular Axons

MARTIN I. SERENO
Committees on Neurobiology and on The Conceptual Foundations of Science, The University of Chicago, Chicago, IL 60637

ABSTRACT

Tectoreticular projections in turtles were examined by reconstructing from serial sections axons that were anterogradely filled with horseradish peroxidase after tectal injections. Three tectoreticular pathways each contain extensively collateralized axons. The crossed *dorsal pathway* (TBd) contains large and small caliber axons. After leaving the tectum, TBd axons emit collaterals into the ipsilateral profundus mesencephali rostralis and then give off a main rostral branch that bears secondary collaterals in the ipsilateral interstitial nucleus of the medial longitudinal fasciculus and the suprapeduncular nucleus. The main trunks cross the midline and descend in the predorsal bundle, generating collaterals at regular intervals. These terminate mostly in the medial half of the reticular core from the midbrain to the caudal medulla. Axons in the uncrossed *intermediate pathway* also emit collaterals into a midbrain reticular nucleus (profundus mesencephali caudalis) and often have a thick rostral branch. The main caudal trunks, however, remain ipsilateral and travel in a diffuse, laterally placed tract, where each emits a long series of collaterals into the lateral half of the reticular core. The uncrossed *ventral pathway* (TBv) contains medium and small caliber axons. TBv axons often have collaterals *within* the tectum and apparently lack main rostral branches. Their caudal trunks run in the tegmental neuropile below the TBi where they collateralize less exuberantly than do TBd and TBi axons.

The morphology of axons in all three pathways suggests that projections from disjunct tectal loci converge at many rostrocaudal levels within the reticular formation. This point was examined explicitly in experiments in which two disjunct injections were placed in one tectal lobe. Intermediate pathway axons traced from the two loci initially formed two distinct bundles but then intermingled in the reticular formation.

Key words: tectum, sensorimotor, reticular formation, non-topographic, eye movements

The optic tectum contains topologically organized afferent maps of the retinal surface (e.g., McIlwain, '75; Graham et al., '81), of auditory space (e.g., Harris et al., '80; Jay and Sparks, '82), and of cutaneous receptors (e.g., Nagata and Kruger, '79; Stein and Gaither, '81). Weakly electric fish, in addition, have a tectal electrosensory map (Bastian, '82) while heat-sensitive snakes have a map of pit organ infared receptors (Hartline et al., '78). There are also inputs of unknown topography from muscle receptors (Abrahams and Rose, '75a,b) and from several vestibular nuclei (Maeda et al., '79).

Electrical stimulation and lesion experiments implicate the tectum in the regulation of orienting movements (Adamük, 1870; Ferrier, 1886; Akert, '49; recent reviews: Wurtz and Albano, '80; Sparks and Mays, '81; Ingle '82; Hartline, '84). The tectum in cats, for instance, appears to initiate coordinated movements of the eyes, head, pinnae, and vibrissae toward spatially localized visual, auditory, and cutaneous target stimuli (Grantyn and Grantyn, '76; Grantyn and Berthoz, '77; Guitton et al., '80; Roucoux et al., '80; Stein and Clamann, '81). The tectum in frogs is involved in the accurate sagittal and horizontal rotation of the body

Accepted October 11, 1984.

Martin Sereno's present address is Division of Biology 216-76, California Institute of Technology, Pasadena, CA 91125. Address reprint requests there.

toward a visual prey stimulus just prior to a tongue flip (Ewert, '70; Grobstein et al., '83). In turtles, the tectum mediates orienting movements of the eyes, neck, and body toward visual stimuli (Bass et al., '73; Bass, '77; Mrosovsky et al., '79).

Thus, the tectum may play a general role in the transformation of topographically organized sensory inputs into the graded motor outputs that underlie orienting movements. A detailed understanding of the organization of tectoreticular pathways linking the tectum to premotor centers in the brainstem reticular formation is essential to an analysis of such orienting behaviors. Previous anatomical studies of tectoreticular neurons have concentrated principally on the laminar distribution of their somata or on the location of tracts and terminal fields. A pattern of tectal efferent projections consistent across vertebrate classes has emerged, including several apparently non-topographic descending pathways that terminate in the reticular formation (e.g., Altman and Carpenter, '61; Rubinson, '68; Kawamura et al., '74; Foster and Hall, '75; Hunt and Künzle, '76; Ulinski, '77; Harting, '77; Harting et al., '80; Smeets, '81; Luiten '81; Burne et al. '81; Huerta and Harting, '82). Information

Abbreviations

BON	Basal optic nucleus
BOT	Basal optic tract
cEnt	Caudal entopeduncular nucleus
CG	Central gray
CM	Caudomedial segment of nucleus rotundus
D	Dorsal hypothalamic nucleus
DC	Dorsal cluster of reticularis inferioris dorsalis
DLA	Dorsolateral anterior nucleus
dLFB	Dorsal peduncle of the lateral forebrain bundle
dLGN	Dorsal lateral geniculate nucleus
dNPC	Dorsal nucleus of the posterior commissure
DMA	Dorsomedial anterior nucleus
EW	Edinger-Westphal nucleus
HP	Habenulopeduncular tract
ICo	Intercollicular nucleus
i-IT	Ipsilateral isthmotectal tract (from Imc)
Imc	Caudal magnocellular nucleus isthmi
Imlf	Interstitial nucleus of the medial longitudinal fasciculus
Imr	Rostral magnocellular nucleus isthmi
Ip	Parvocellular nucleus isthmi
Ipd	Dorsal interpeduncular nucleus
Ipv	Ventral interpeduncular nucleus
LHA	Lateral hypothalamic area
LM	Nucleus lentiformis mesencephali
Mes V	Mesencephalic trigeminal nucleus
MFB	Medial forebrain bundle
MLF	Medial longitudinal fasciculus
nLL	Nucleus of the lateral lemniscus
Nmlf	Nucleus of the medial longitudinal fasciculus
N. III	Oculomotor nerve
N. IV	Trochlear nerve
N.V	Trigeminal nerve
N. VIII	Auditory-vestibular nerve
N. IX	Glossopharyngeal nerve
OT	Optic tract
P	Periventricular hypothalamic nucleus
Pa	Paraventricular hypothalamic nucleus
PC	Posterior commissure
PD	Nucleus posterodorsalis of the pretectum
Pe	External pretectal nucleus
PMc	Profundus mesencephali caudalis
PMr	Profundus mesencephali rostralis
PMrl	Profundus mesencephali rostrolateralis
PMr-Tect	PMr-tectal tract
PMv	Profundus mesencephali ventralis
Po	Posterior hypothalamic nucleus
PR	Prerubral area
Pt	Nucleus pretectalis
Re	Nucleus reuniens
rEnt	Rostral entopeduncular nucleus
Ri	Inferior raphe nucleus
RID	Reticularis inferioris dorsalis
RM	Reticularis medius
RML	Reticularis medius lateralis
RN	Red nucleus
Rot	Nucleus rotundus
RSL(dm)	Reticularis superioris lateralis, dorsomedial segment
RSL(vl)	Reticularis superioris lateralis, ventrolateral segment
Rsl	Lateral superior raphe nucleus
RSM	Reticularis superioris medius
Rsm	Medial superior raphe nucleus
SAC	Stratum album centrale
SC	Small-celled nucleus
SFGS	Stratum fibrosum et griseum superficiale
SGC	Stratum griseum centrale
SGP	Stratum griseum periventriculare
SN	Substantia nigra
SN pr	Substantia nigra pars reticulata
SO	Stratum opticum
SP	Suprapeduncular nucleus
SpO	Superior olive
TBd(lg)	Dorsal tectobulbar pathway, large caliber component
TBd(sm)	Dorsal tectobulaar pathway, small caliber component
TBi	Intermediate tectobulbar pathway
TBv(med)	Ventral tectobulbar pathway, medium caliber component
TBv(sm)	Ventral tectobulbar pathway, small caliber component
Tect-Imc	Tectoisthmi tract (to Imc)
Torc	Torus semicircularis, central nucleus
Torl	Torus semicircularis, laminar nucleus
TTh	Tectothalamic tract
V	Ventral thalamic nucleus
VeDL	Dorsolateral vestibular nucleus
vEnt	Ventral entopeduncular nucleus
VEO	Ventricular ependymal organ
VeVL	Ventrolateral vestibular nucleus
VeVM	Ventromedial vestibular nucleus
vLFB	Ventral peduncle of the lateral forebrain bundle
VL	Ventrolateral thalamic nucleus
VM	Ventromedial thalamic nucleus
VMH	Ventromedial hypothalamic nucleus
VTA	Ventral tegmental area
x-IT	Crossed isthmotectal tract
x-SC-Tect	Crossed SC-tectal tract
x-TBd	Contralateral part of the dorsal pathway
x-TTH	Crossed tectothalamic tract
x-Ve-Tect	Crossed vestibulotectal tract (from VeVL)
III	Oculomotor nucleus
IV	Trochlear nucleus
V ds	Descending trigeminal nucleus
V mot	Trigeminal motor nucleus
V mr	Mesencephalic root of the trigeminal nerve
V pr	Principal sensory trigeminal nucleus
V tr	Descending tract of the trigeminal complex
VI	Abducens motor nucleus
VII	Facial motor nuccleus
XII	Hypoglossal motor nucleus

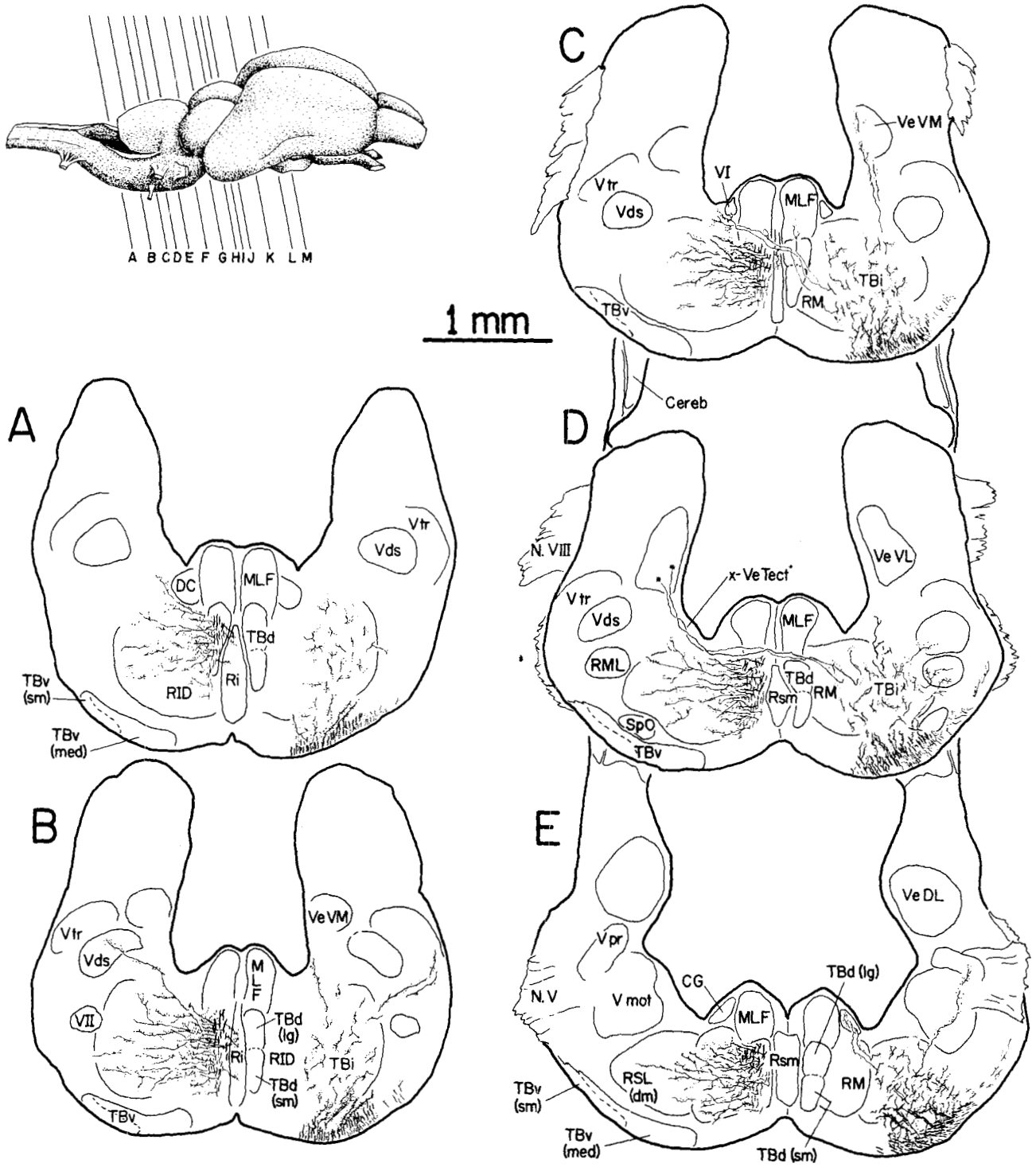

Fig. 1. Drawings of fibers labeled by a large injection of HRP into the right tectum. The planes of sections A–E are indicated on the brain in inset (which also locates sections for figs. 2 and 3). On the contralateral (left) side, the crossed *dorsal tectobulbar pathway* (TBd) courses near the midline emitting collaterals into the medial reticular formation. On the ipsilateral (right) side, the *intermediate tectobulbar pathway* (TBi) courses through the lateral half of the reticular core while the *ventral tectobulbar pathway* (TBv) travels along the ventrolateral surface of the brainstem directly under the intermediate pathway. Retrogradely labeled tracts (marked with an asterisk) include the crossed vestibulotectal input (x-Ve Tect). Some of the longer fibers shown were reconstructed from several adjacent sections. Retrogradely labeled cells (not shown) were found in RSL(vl), VeVL, and RID.

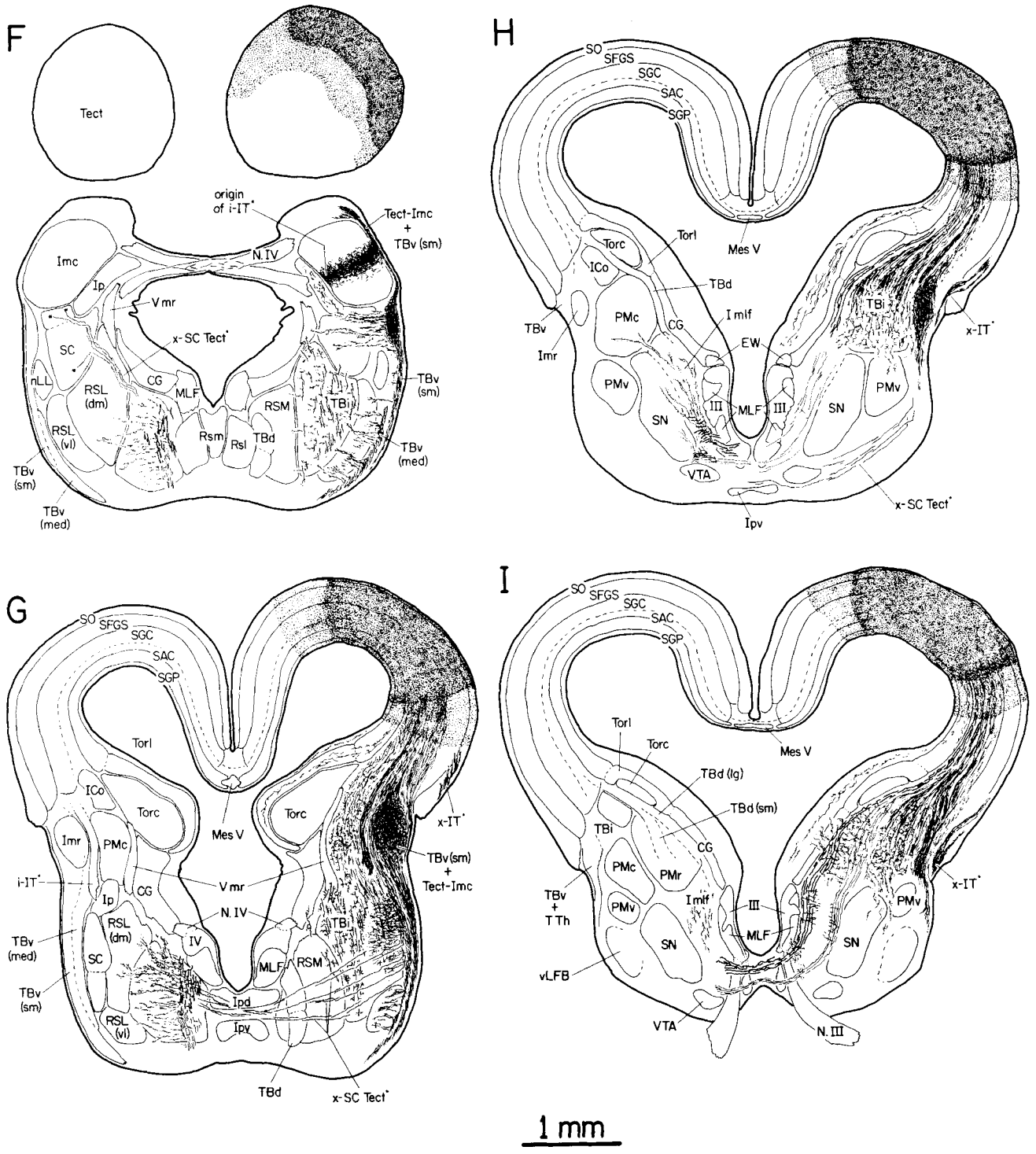

Fig. 2. Drawings of fibers labeled by a large unilateral HRP injection. See Figure 1 for location of section planes. The dorsal, intermediate, and ventral tectobulbar pathways can all be seen leaving the tectum in section I. The *dorsal pathway* (TBd) emits rostrally directed ipsilateral branches (see also Fig. 3) before decussating (section I) and turning caudally to run just lateral to the midline of the tegmentum in sections H, G, and F. The *intermediate* (TBi) and *ventral* (TBv) *pathways* emerge caudal to the dorsal pathway (sections H and G) and remain ipsilateral to the injection for their entire course. The densely labeled tectoisthmi pathway (Tect-Imc, section F) is also illustrated. Retrogradely labeled tracts (marked with asterisks) include the ipsilateral isthmotectal tract (i-IT, from Imc), the crossed isthmotectal tract (x-IT), and the crossed tract from SC (x-SC Tect). Retrogradely labeled cells (not shown) were found in isthmic (SC, Imc, Ip, Imr) and mesencephalic (ICo, Torl, SN, PMc, PMr) nuclei.

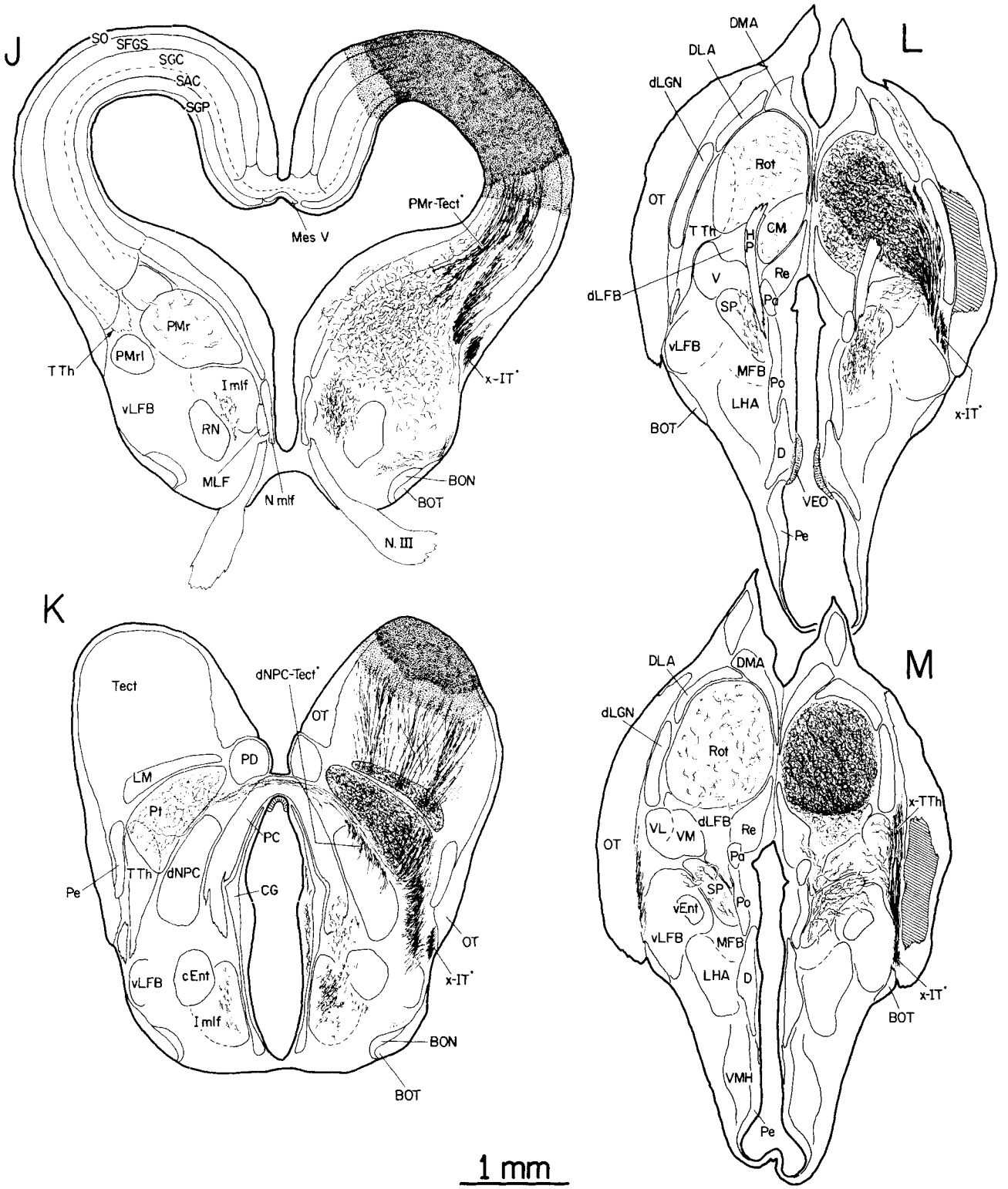

Fig. 3. Drawings of fibers labeled by a large unilateral HRP injection. For location of section planes see Figure 1. A dense mat of collaterals from dorsal pathway axons occupies the midbrain nucleus profundus mesencephali rostralis (PMr, section J; see also Fg. 4C). Further ventrally, dorsal pathway axons also give off "main rostral collaterals" that pass just medial to the red nucleus (section J) and just lateral to the large cells in the interstitial nucleus of the medial longitudinal fasciculus (Imlf, section K) to eventually terminate in the suprapeduncular nucleus (SP) of the ventral thalamus (sections L and M). The densely labeled *tectopretectal pathway* (emitted from injection site in section K), which projects to lentiformis mesencephali (LM) and a region dorsal to dLGN, and the *tectorotundal pathway* (TTh), which projects to nucleus pretectalis (Pt), the nucleus of the TTh (nTTh), and nucleus rotundus (Rot), are also illustrated. Retrogradely filled axons in the optic tract are indicated by hatching. Other retrogradely labeled tracts (marked with asterisks) include PMr-tectal axons (PMr-Tect), the ipsilateral bundle from the dorsal nucleus of the posterior commissure (dNPC-Tect), and the crossed isthmotectal tract (x-IT). Retrogradely labeled cells (not shown) were found in mesencephalic (PMr, PMrl), pretectal (Pt, LM, Pe, dNPC), and diencephalic (cEnt, V) nuclei. Finally, retinal terminals in dLGN and Pe filled through their tectal branches are omitted in sections K–M.

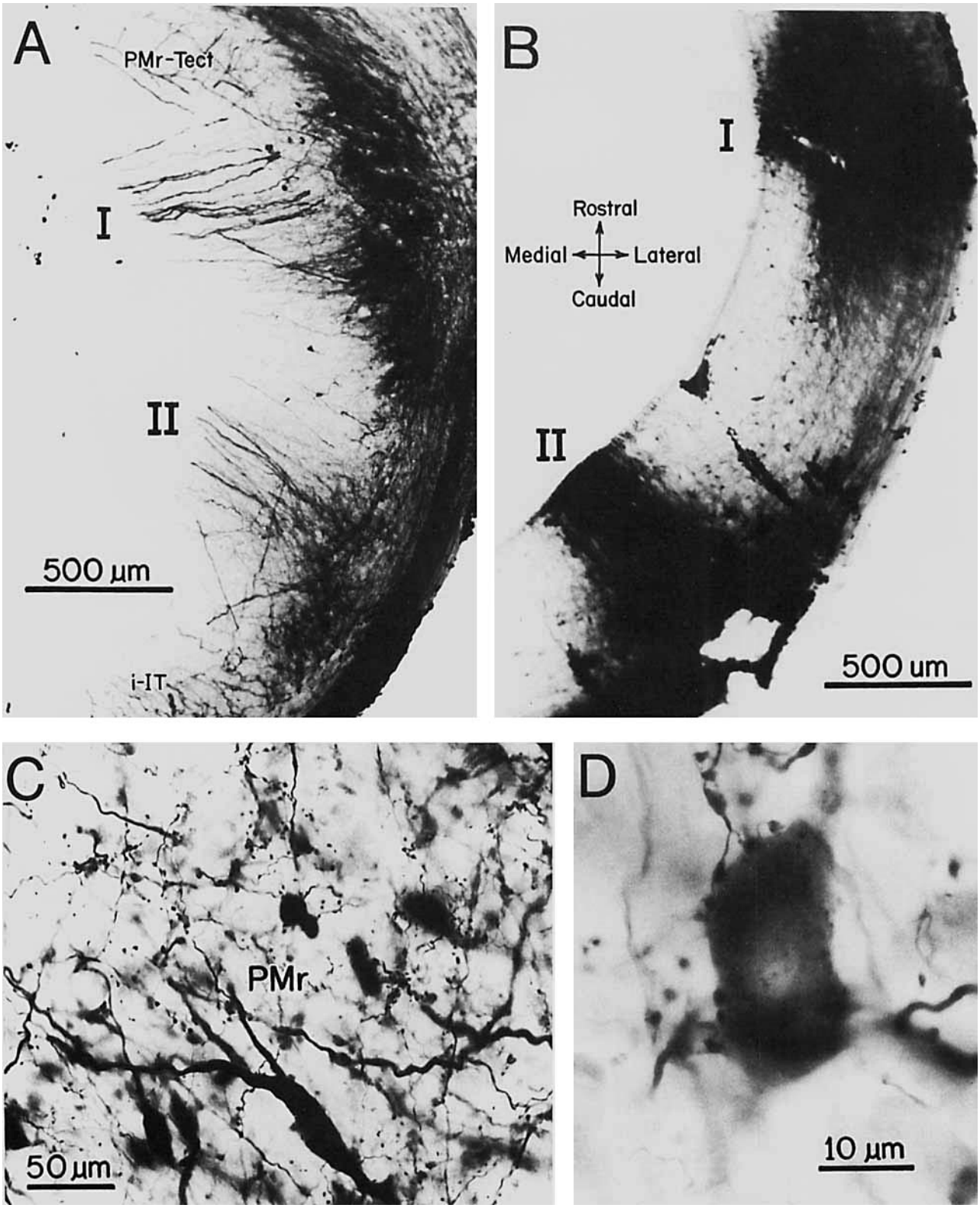

Fig. 4. Photomicrographs of injection sites and HRP-filled neurons. Two small tectal injection sites (I, II) in the horizontal section in B each emit thin bundles of tectobulbar axons apparent several sections ventrally in A. The retrogradely labeled tracts from profundus mesencephali rostralis (PMr-Tect) and the caudal magnocellular nucleus isthmi (i-IT) are also visible in A. C is a transverse view of the dorsal pathway terminal field in profundus mesencephali rostralis (PMr) (see Fig. 3J) labeled after an extensive tectal HRP injection. The injection also back-filled large PMr cells which have long, sparsely branched dendrites arrayed in the transverse plane. D is a high-magnification view of a putative contact between solid-filled boutons from a dorsal pathway axon and the soma of a lightly back-filled PMr cell.

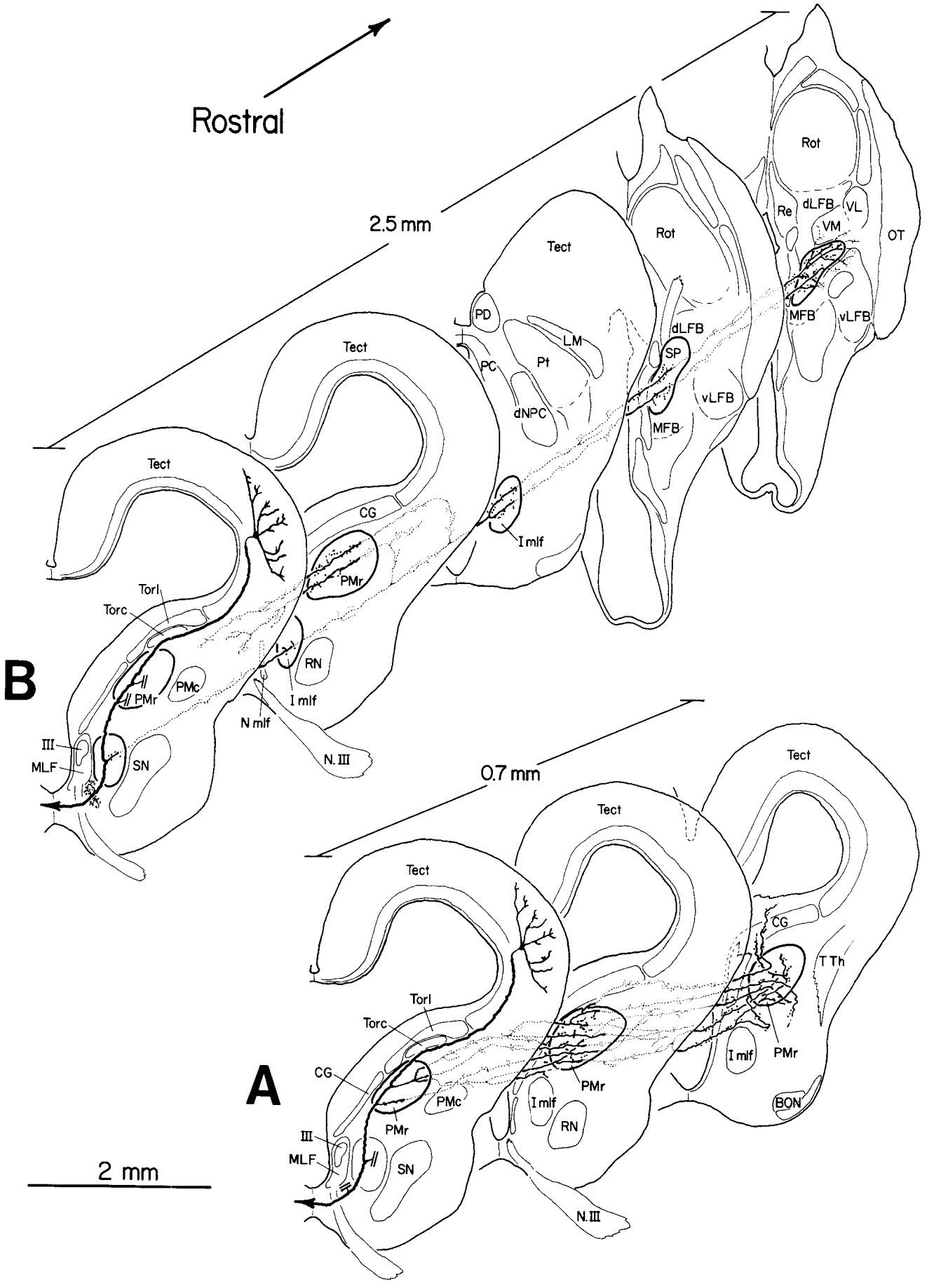
Rostral
2.5 mm
Tect
Rot
Re
dLFB
VL
VM
OT
PD
LM
PC
Pt
SP
MFB
vLFB
dNPC
CG
PMr
Torl
Torc
RN
PMc
I mlf
N mlf
III
MLF
SN
N. III
B
0.7 mm
TTh
BON
A
2 mm

Figure 5

on the detailed organization of the tectoreticular pathways, by contrast, is just beginning to appear (Grantyn and Grantyn, '82; Grantyn et al., '82; Dacey '82).

The present study examines the morphology of tectoreticular axons at the single-cell level by using small extracellular horseradish peroxidase (HRP) injections and serial section reconstruction techniques. The following paper (Sereno and Ulinski, '85) illustrates the morphology of the dendrites of tectoreticular neurons and discusses the results in the light of current ideas about the nature of the sensorimotor transformation underlying tectally mediated orienting movements.

MATERIALS AND METHODS

Twenty-five pond turtles (*Pseudemys scripta elegans* and *Chrysemys picta*) weighing 0.5–1.5 kg were used. Animals were anesthetized with a small (0.3 ml/kg) dose of Brevital (Wang et al., '77) and packed in ice for surgery. This technique provides stable anesthesia and a helpful reduction in blood pressure. A craniotomy was performed, and either a 1 μl Hamilton syringe with a sharpened tip or a micropipette was introduced into the tectum. In nine animals, multiple pressure injections (total of 0.2–0.8 μl) or iontophoretic injections (2–4 μA for 20 minutes at each site) of concentrated Sigma Type VI HRP in pH 8.6 Tris buffer were made at two to four sites in one tectal hemisphere. Thirteen other animals received small iontophoretic injections (1 μA pulsed for 20–100 seconds with a 5–10 μm I.D. tip) at a single site or at two widely separated sites. Three animals received unilateral subtotal tectal lesions.

Animals with HRP injections survived for 3 days at 20°C before intracardial perfusion with pH 7.4 phosphate-buffered saline followed by a buffered solution of 1% paraformaldehyde and 3% glutaraldehyde. Brains were removed, soaked in 30% sucrose, embedded in gelatin, and sectioned the next day on a freezing microtome at 110 or 120 μm. Transverse and horizontal serial sections were processed according to the cobalt-enhanced diaminobenzidine method of Adams ('77). The gelatin was removed and sections were carefully aligned on slides to facilitate serial reconstructions. Sections were usually counterstained with cresyl violet before coverslipping. In other cases, reconstructions were done from unstained sections and the coverslips were removed for counterstaining afterward.

Sections shrunk significantly during drying. When cut at 120 μm they often ended up only 45 μm thick (60–65% shrinkage) as measured by a stage micrometer under oil. Shrinkage in directions parallel to the plane of section was much less (0–5%), apparently because the section becomes bonded to the slide before it dries. This anisotropy in shrinkage results in an artifactual "crumpling" of axons perpendicular to the slide not seen in Golgi preparations where the tissue is infiltrated with a supporting medium before sectioning. Since tectobulbar axons tend to travel and emit collaterals in a horizontal plane, most single axon reconstructions were done from horizontal sections to minimize this artifact.

Low-power chartings of the distribution of efferents labeled by large injections were made with a drawing tube. Axons were drawn semischematically at about four times actual diameter to illustrate their morphology better. Single HRP-filled axons were reconstructed with a drawing tube from a number of adjacent sections under a 100× oil objective to illustrate their detailed morphology. This magnification resulted in very large drawings but was necessary to distinguish closely apposed processes within a section. Slight color differences were also helpful in this regard. The tendency for cut ends of filled axons to be darkly stained at the surfaces of a section (perhaps due to better access to the staining solutions) greatly facilitates locating a process in adjacent sections and even fine branches could be confidently traced. To locate a process in the adjacent section, a drawing tube and a 16× objective were first used to mark down the exit diameters and directions of labeled axons in the current section (including the target axon and several surrounding axons) on a scratch sheet. Then, while viewing the proper surface of the next section, the scratch sheet was moved under the drawing tube until the appropriate pattern of axon diameters and directions was detected. In most cases, the target axon could be located in a few seconds; with crowded fields, it was sometimes necessary to repeat the procedure at a higher magnification. The reconstruction process was most practical when less than 20 main axon trunks were labeled in a given pathway; consequently, injections for a single axon reconstructions were usually less than 250 μm in diameter (under 1% of the tectal surface). Low-power tracings of sections containing reconstructed axons were done with a drawing tube. Since a single section usually contained only disconnected segments of a given axon, a reconstructed portion made from up to five sections was photographically reduced to the appropriate dimensions and superimposed on a low-power tracing of a single section whenever the surrounding structures had borders approximately perpendicular to the plane of section.

A stereodiagram was made by hand (Glenn and Burke, '81) from sixteen 110 μm serial, horizontal sections for one of the double injection cases. Main tectoreticular axon trunks in each section were traced at 190× total magnification (16× objectve). A disparity of 1 mm per section (at 190×) was then introduced, resulting in some compression of the depth axis but allowing the entire reconstruction to be displayed in one panel. The stereodiagram can be viewed by ocular deviation or by using a standard stereoviewer.

The nomenclature of cell groups and fiber tracts generally follows Cruce and Nieuwenhuys ('74) and ten Donkelaar and Nieuwenhuys ('79). Nomenclature for the brainstem reticular fields follows Newman et al. ('83), while that for rostral midbrain and thalamic structures follows Papez ('35) as modified by Rainey ('78), Balaban and Ulinski ('81), and Bass and Northcutt ('81). The identification of the substantia nigra and surrounding structures was based on the histochemical studies of Parent ('79) and Brauth et al. ('83). The tectal lamination scheme is from Huber and Crosby ('33) except that layer 8 of Ramón (1896) has been included in the central gray. Several new midbrain tegmental cell groups and fiber tracts were identified and named in the present study.

Fig. 5. Schematic summary of the ipsilateral collaterals of a dorsal pathway axon. The first branches shown in A arborize in the midbrain nucleus profundus mesencephali rostralis (PMr). In B, the PMr branches have been removed to better illustrate the "main rostral collateral." It first courses under PMr sending branches up into PMr, and then continues through the interstitial nucleus of the medial longitudinal fasciculus (Imlf) to end in the suprapeduncular nucleus (SP) of the ventral thalamus. Small clumps of boutons arise throughout its course. The main trunk crosses the midline to run in the contralateral predorsal bundle.

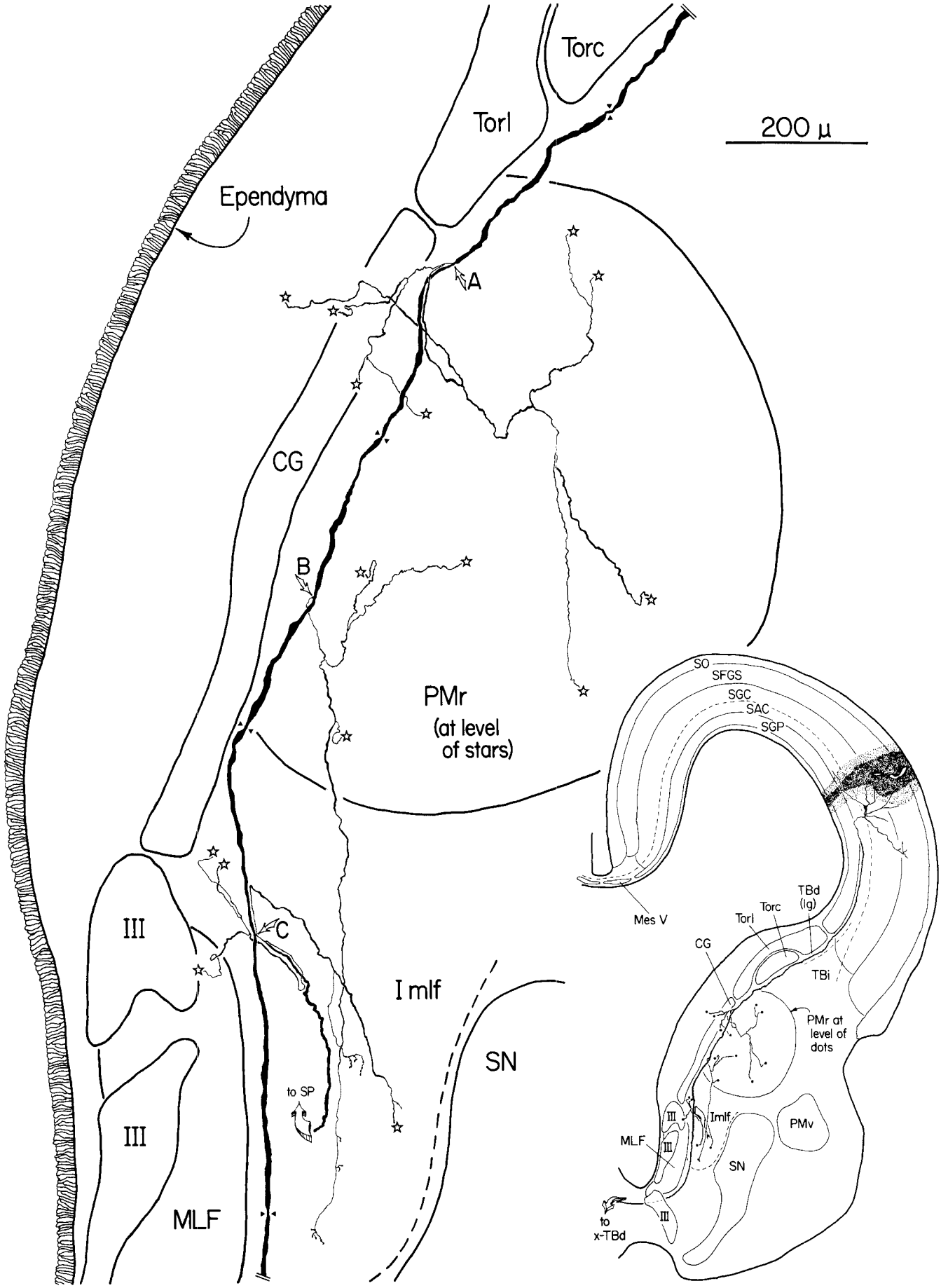
Torc
Torl
200 μ
Ependyma
A
CG
B
PMr
(at level
of stars)
III
C
I mlf
SN
to SP
III
MLF
SO
SFGS
SGC
SAC
SGP
Mes V
TBd
(lg)
Torc
Torl
CG
TBi
PMr at
level of
dots
III
Imlf
PMv
MLF
III
SN
III
to
x-TBd

Figure 6

RESULTS

The results are divided into three parts. First, a transversely sectioned case with a large injection is illustrated and described to demonstrate the overall organization of the three tectoreticular pathways. Second, examples of single axons from each pathway are described on the basis of serial reconstructions, principally from horizontal sections. Finally, the results of a double injection experiment designed to directly examine the convergent nature of the tectoreticular projections are presented.

Organization of tectoreticular pathways

There are three tectoreticular pathways in pond turtles—a *dorsal pathway* (TBd) with large and small caliber components, a medium caliber *intermediate pathway* (TBi; a key to nomenclature abbreviations precedes Fig. 1), and a *ventral pathway* (TBv), with medium and small caliber components. These pathways are illustrated in Figures 1–3. A large HRP injection in this case had an effective uptake zone covering 30–40% of the tectal surface as judged by the extent of label in the optic tract (marked by hatching in Fig. 3L,M) and by the restricted band of label in the topographically organized caudal magnocellular nucleus isthmi (Fig. 2F). Pathways and nuclei are sometimes identified on the unlabeled side to avoid covering up labeled axons.

Dorsal tectobulbar pathway (TBd). Axons forming this pathway travel deep in the stratum album centrale (SAC), exit the tectum as a sheet about 100 μm thick and 800 μm long, and pass lateral to the central nucleus of the torus semicircularis (Torc) before dividing into a medial, large caliber (4–6 μm) and a lateral, small caliber (1–2 μm) component (Fig. 2I). The rostral edges of these components encroach on the caudal pole of the large-celled profundus mesencephali rostralis (PMr). Both components emit collaterals into this nucleus as they pass behind it (Figs. 3J, 4C). A few collaterals reach the small-celled profundus mesencephali rostrolateralis (PMrl, Fig. 3J) while others encroach on the central gray as well as the cell-free zone medial to it. The collaterals in profundus mesencephali rostralis continue forward and end ventral to the dorsal nucleus of the posterior commissure (dNPC) at the caudal face of the diencephalon (Fig. 3K).

The main trunks of large and small TBd axons continue ventrally between the substantia nigra and the medial longitudinal fasciculus where robust collaterals arise (Fig. 2I) and travel rostrally through the interstitial nucleus of the medial longitudinal fasciculus (Imlf, = interstitial nucleus of Cajal) emitting secondary collaterals and terminals (Fig. 3J,K). The main collaterals continue rostrally into the suprapeduncular nucleus (SP, Fig. 3L) emitting terminals and abruptly turning laterally to end at mid-rotundal levels (Fig. 3M).

The main trunks next cross the midline, passing through both oculomotor nerves, and then turn caudally to form the paramedian predorsal bundle just ventral to the medial longitudinal fasciculus. The small caliber axons remain ventral to the large caliber axons throughout the brainstem. A few robust collaterals are emitted rostrally into the contralateral interstitial nucleus of the medial longitudinal fasciculus soon after the main trunks turn caudally. These eventually reach the SP to form a small contralateral complement of a predominantly ipsilateral rostral pathway. Profundus mesencephali rostralis also receives a small contralateral projection from TBd at this level.

Larger numbers of collaterals begin arising from both components at the level of the trochlear nucleus. The initial branches follow the upward sweep of the rostral parts of reticularis superioris medialis (RSM) and the dorsomedial segment of reticularis superioris lateralis (RSL(dm)) (Fig. 2F,G). The majority terminate in reticularis superioris medialis, but some collaterals extend into the dorsomedial segment of reticularis superioris lateralis and a small-celled nucleus (SC) located ventral to the caudal magnocellular nucleus isthmi (Imc) (Fig. 2F). As the main trunks of TBd axons continue caudally, their collaterals have less of a tendency to curve dorsally. These branches extend 500–800 μm into the reticular core, forming a rather sparse terminal zone within the medial half of reticularis medius (RM) and reticularis inferioris dorsalis (RID) (Fig. 1A–E). Some TBd collaterals reach the spinal trigeminal nucleus while others are emitted medially into the raphe (Fig. 1A,B) just caudal to the level where very large cells are seen in the inferior raphe nucleus (Ri). Staining faded in the caudal medulla while the main trunks were still thick (4–5 μm for the large component), suggesting that these axons were not completely filled. Consequently, it was not possible to determine if any TBd axons project to the spinal cord.

In summary, TBd axons have a widespread distribution to medial "reticular" structures from the diencephalon to the caudal medulla. The only apparent difference between small and large caliber components is size; their overall distributions are remarkably similar.

Intermediate tectobulbar pathway (TBi). The TBi pathway resembles the TBd pathway, but is primarily ipsilateral and is more laterally placed. Medium caliber (1.5–2.5 μm) axons in this pathway travel in the middle layers of the stratum album centrale, leave the tectum in a diffuse bundle lateral to the TBd sheet, and bend laterally along with the TBd as it divides into large and small components (Fig. 2I). The TBi bundle turns caudally after leaving the tectum, emitting a mass of terminals in profundus mesencephali caudalis (PMc) that extends to the central gray in sections caudal to profundus mesencephali rostralis. Collaterals arise as TBi axons course near or through the intercollicular nucleus (ICo, a target of the spinal cord—Künzle and Woodson, '82). There appears to be little overlap between the TBi projection to profundus mesencephali caudalis (and ICo) and the TBd projection to profundus mesecephali rostralis (Figs. 2H,I, 3J). A few TBi fibers also project to the large-celled profundus mesencephali ventralis (PMv, = "nucleus profundus mesencephali" of Papez, '35; Brauth et al., '83) (Fig. 2H). Single-axon reconstructions

Fig. 6. Partial reconstruction from transverse sections of the ipsilateral collaterals of a dorsal pathway neuron. A large tectal neuron (see inset) was filled through a distal dendrite. It gives off a robust axon that courses just behind profundus mesencephali rostralis (PMr) in the large caliber component of the dorsal pathway, eventually crossing to run in the predorsal bundle. The first two collaterals at A and B course rostrally (into the picture) to enter PMr. They branch almost immediately, spanning the dorsoventral extent of PMr. Stars indicate where each branch leaves the rostral-most section used for the reconstruction; the outline of PMr is taken from that level. Many preterminal branches bearing small clumps of boutons are subsequently given off (not shown). The "main rostral collateral" arises at C as the main trunk passes the oculomotor nucleus. Collateral C continues rostrally for several millimeters, eventually reaching the suprapeduncular nucleus. Nodes without collaterals are indicated by small pairs of filled triangles.

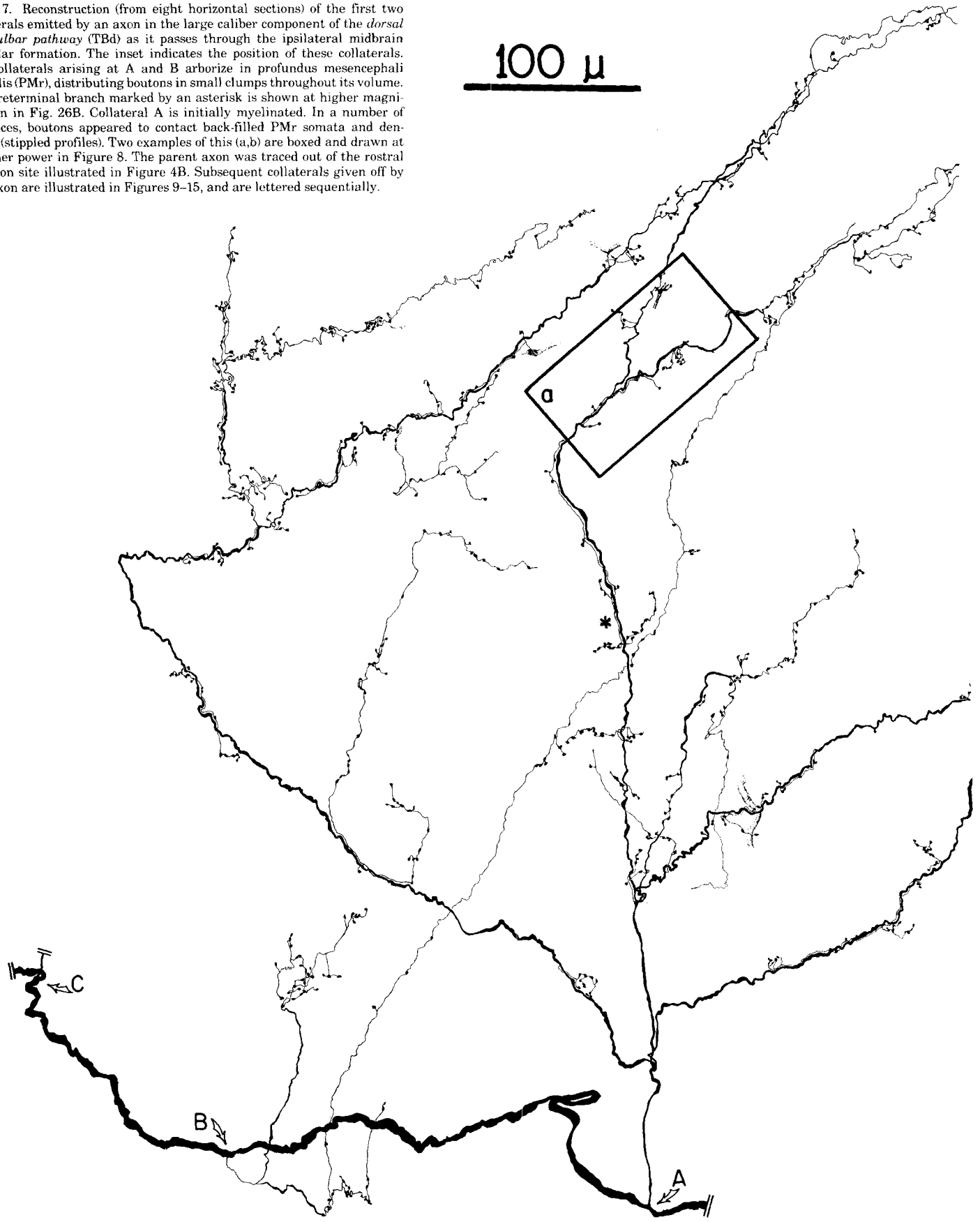

Fig. 7. Reconstruction (from eight horizontal sections) of the first two collaterals emitted by an axon in the large caliber component of the *dorsal tectobulbar pathway* (TBd) as it passes through the ipsilateral midbrain reticular formation. The inset indicates the position of these collaterals. The collaterals arising at A and B arborize in profundus mesencephali rostralis (PMr), distributing boutons in small clumps throughout its volume. The preterminal branch marked by an asterisk is shown at higher magnification in Fig. 26B. Collateral A is initially myelinated. In a number of instances, boutons appeared to contact back-filled PMr somata and dendrites (stippled profiles). Two examples of this (a,b) are boxed and drawn at a higher power in Figure 8. The parent axon was traced out of the rostral injection site illustrated in Figure 4B. Subsequent collaterals given off by this axon are illustrated in Figures 9–15, and are lettered sequentially.

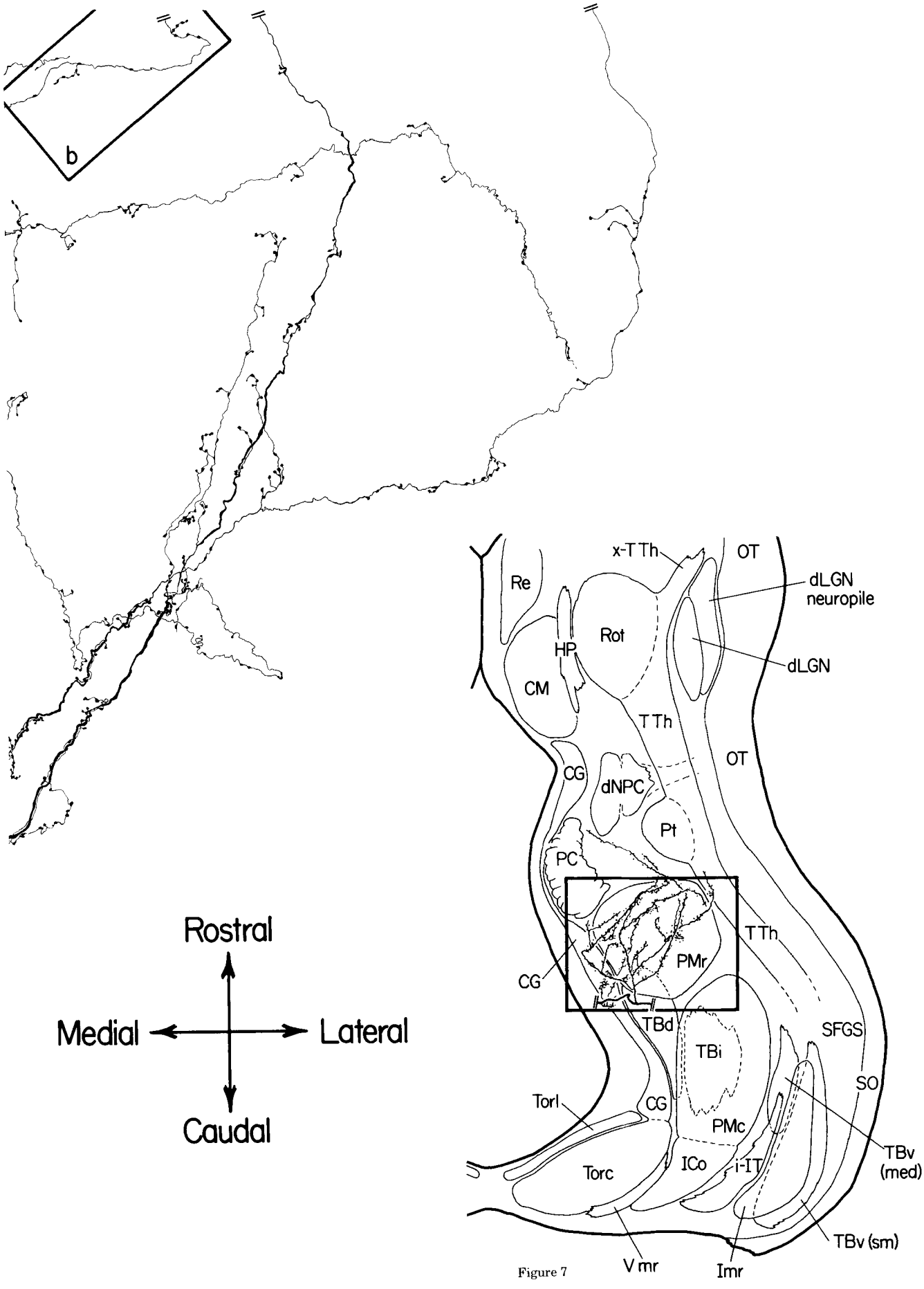
b
Rostral
Medial
Lateral
Caudal
x-T Th
OT
Re
dLGN
neuropile
Rot
HP
dLGN
CM
T Th
OT
CG
dNPC
Pt
PC
T Th
PMr
CG
TBd
SFGS
TBi
SO
Torl
CG
PMc
TBv
(med)
Torc
ICo
i-IT
TBv (sm)
V mr
Imr

Figure 7

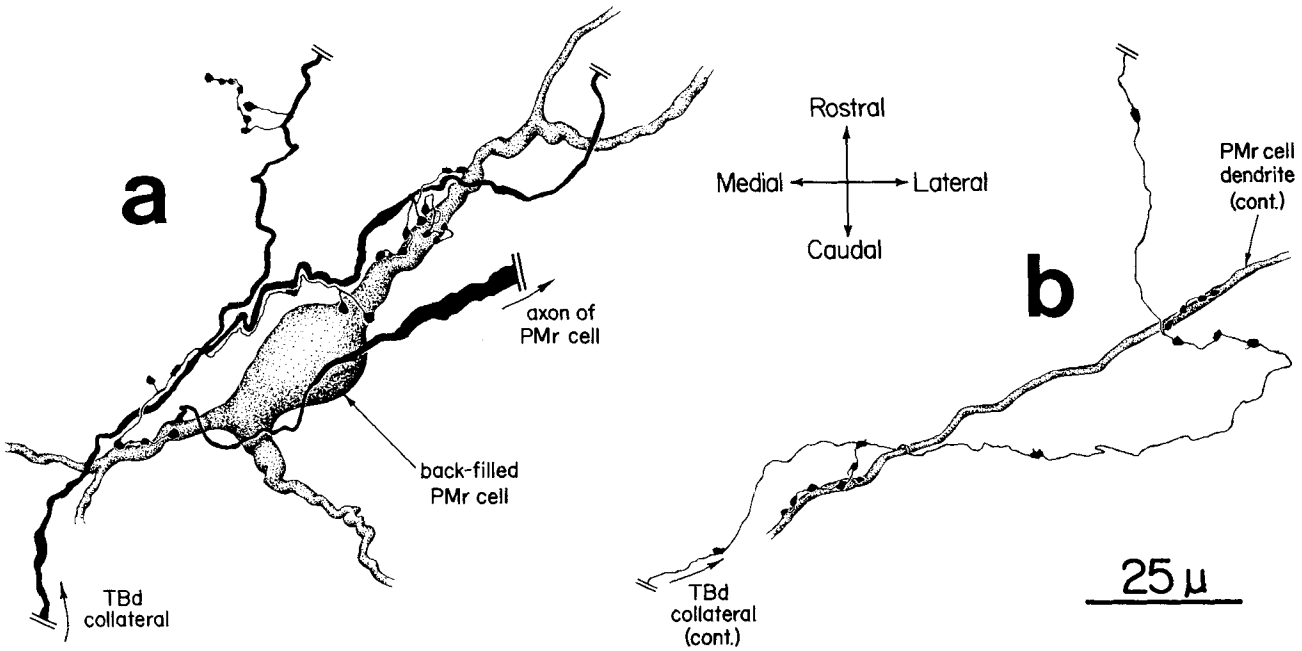

Fig. 8. High-power views of boxed regions in Figure 7. In a, two preterminal branches given off by a myelinated dorsal pathway (TBd) collateral make 14 apparent contacts with the proximal dendrites of a back-filled profundus mesencephali rostralis (PMr) cell while in b, another preterminal branch from the same collateral makes nine more apparent contacts with a distal dendrite of the same cell.

reveal thick collaterals of TBi axons that arise at the level of profundus mesencephali caudalis and pass rostrally through the TBd, afterward penetrating the central gray to run rostroventrally in its medial neuropile to the caudal diencephalon (Fig. 3K).

Moving caudoventrally, the main caudal trunks of TBi axons pass into the rostral pole of the dorsomedial segment of reticularis superioris lateralis emitting regular branches. Some very fine collaterals enter the contiguous SC (= "nucleus of the lateral lemniscus" of Cruce and Nieuwenhuys, '74) at this level. The tract then runs through or just lateral to the magnocellular elements that appear caudally in the dorsomedial segment of reticularis superioris lateralis. Many collaterals at this and more caudal levels turn medially, although they usually avoid entering deeply into the medial TBd terminal field. Continuing caudally, TBi axons give off collaterals that occupy the lateral halves of reticularis medius and then reticularis inferioris dorsalis (Fig. 1A–E). A few ipsilateral TBi collaterals reach the caudal central gray (Fig. 1E), a vestibular nucleus (VeVM), and the trigeminal complex, while others arborize in the Ri or cross the midline dorsal to the TBd and arborize near the contralateral abducens nucleus (Fig. 1C). The main trunks of TBi axons were visible further caudally than TBd axons since they do not decussate. In contrast to TBd axons, most had thinned to less than half their original diameters by the time they entered reticularis inferioris dorsalis. Although the main trunks of TBi axons do not form a tight bundle, they remain dorsal to the ventral pathway (TBv) throughout their trajectory. A few large axons (4–5 μm) were present among the medium caliber axons of the TBi. When followed through serial sections, a number of these turned out to be retrogradely labeled axons of large neurons in the contralateral ventrolateral vestibular nucleus (Fig. 1D).

Ventral tectobulbar pathway (TBv). The ventral tectobulbar pathway contains small and medium caliber axons that travel in the more superficial layers of the SAC. Small caliber TBv axons also travel in a thinner fiber layer near the top of the stratum griseum centrale (SGC). TBv axons leave the tectum lateral to the TBi band and divide into a medially placed medium caliber component (2.5–3.5 μm) and a more lateral, small caliber component (1 μm or less). Immediately after leaving the tectum, the small caliber component of the TBv enters the retrogradely labeled rostral magnocellular nucleus isthmi (Imr, = "profundus mesencephali" of Foster and Hall, '75) where it swells into an almond-shaped mass of fine fibers and small and large boutons (Fig. 2G). A tract that travels with the TBv(sm) as it leaves the tectum is the ipsilateral tectoisthmi tract (Tect-Imc, Fig. 2F,G). Caudal to rostral magnocellular isthmi, the medium caliber axons of the tectoisthmi tract become distinguishable as they separate medially from TBv(sm) and begin entering the rostrolateral surface of caudal magnocellular isthmi (Fig. 2F). The medium caliber component of the TBv runs just medial to rostral magnocellular isthmi (Figs. 2F,G, 20, 21). Finally, there is a small unnamed efferent tract (seen also in lesion cases) that issues from the rostrolateral face of the rostral magnocellular isthmi complex (ventrolateral-most fibers in Fig. 2I). At the level of the basal optic nucleus, medially directed collaterals arise from it (Fig. 3J,K) and enter the cell-poor zone of the tegmentum that overlies the basal optic nucleus.

Soon after TBv(sm) emerges from rostral magnocellular isthmi, and TBv(med) passes the medial edge of that nucleus, the tracts condense into distinct lateral and medial bundles. At this level, both give off fine, medially directed collaterals that give rise to a terminal field in the SC in the dorsolateral mesencephalic tegmentum. That nucleus begins rostrally just behind the large-celled profundus mesencephali ventralis (Fig. 2G) and ends under the middle of the caudal magnocellular isthmi. The two TBv components give off collaterals only to the dorsal half of the SC; the ventral half characteristically contains cell clusters that are not seen among the evenly spaced cells of the dorsal half. TBv(sm) in addition gives off a sheet-like terminal zone embedded in the pathway itself that is especially dense in the neuropile lateral to the caudal part of that nucleus (Fig. 2F).

A number of *retrogradely* labeled tracts enter the tectum near the exit of the *anterogradely* labeled TBv(med) and TBv(sm), and it was important to clearly distinguish these two types of labeling. Before continuing, then, the retrogradely labeled tracts will be described, starting with the most lateral. The thin band of fibers lateral to TBv(sm) in the stratum opticum (SO) in Figure 2H is the retrogradely labeled crossed isthmotectal tract (x-IT). Traced out of the tectum, it joins the anterogradely labeled crossed tectorotundal tract in the thalamus (x-TTh in Fig. 3M). Both tracts eventually cross in the supraoptic decussation. Second, the large neurons in rostral magnocellular isthmi project to the tectum via the TBv(sm). Third, the retrogradely labeled ipsilateral isthmotectal tract (i-IT) has a complex relationship with the more medially located component of the TBv. The i-IT is a distinct axon bundle that arises from the rostromedial face of caudal magnocellular isthmi, makes a sharp, dorsal turn, and courses toward the tectum (Figs. 2G, 19), which it enters to run in the upper part of the stratum griseum centrale *superficial* to TBv(med) axons in the stratum album centrale. As the TBv(med) runs past the rostral magnocellular isthmi, it must therefore pass through the i-IT to reach the lateral surface of the brainstem. Finally, there is a small bundle of large caliber axons that crosses between the dorsal and ventral interpeduncular nuclei (x-SC Tect in Fig. 2G,H) and enters the tectum within the medium caliber component of the TBv. These turned out to be retrogradely labeled axons of crossed tectal-projecting cells located in the caudal parts of the SC ventral to the caudal magnocellular isthmi. Recently, Schnyder and Künzle ('83) back-labeled cells in the SC after contralateral intraocular injections in turtles. It seems possible, in view of their results, that some of the labeled cells in that nucleus in the present material are in fact retinal-projecting neurons whose axons were interrupted by the large injection as they passed through the tectum en route to the optic tract and retina. The lateral to medial sequence at the level of rostral magnocellular isthmi, then, is (1) x-IT, (2) TBv(sm) plus Tect-Imc, (3) TBv(med) plus i-IT plus x-SC Tect, and (4) TBi.

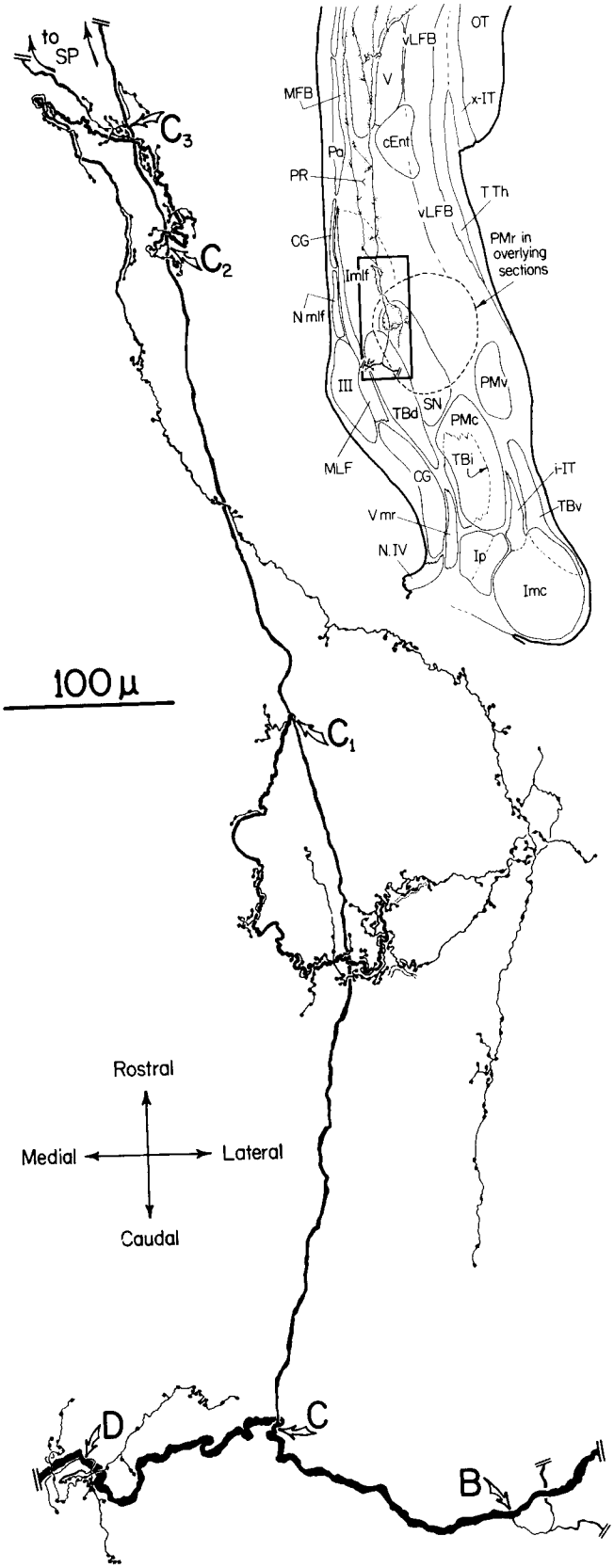

Fig. 9. Reconstruction from seven horizontal sections of the third and fourth collaterals emitted by the main TBd axon trunk shown in Figure 7. The collateral arising at C is the myelinated "main rostral collateral" seen on all TBd axons. It arises as the parent trunk passes between the oculomotor nucleus and the substantia nigra. As collateral C passes beneath profundus mesencephali rostralis (PMr), it emits two secondary collaterals (at C_1 and C_2) that travel vertically for about 700 μm to reach PMr, where they arborize among the preterminal branches shown in Figure 7. The small collateral at D arborized near the oculomotor nucleus. The inset shows the location of the high-power view as well as the location of PMr in overlying sections.

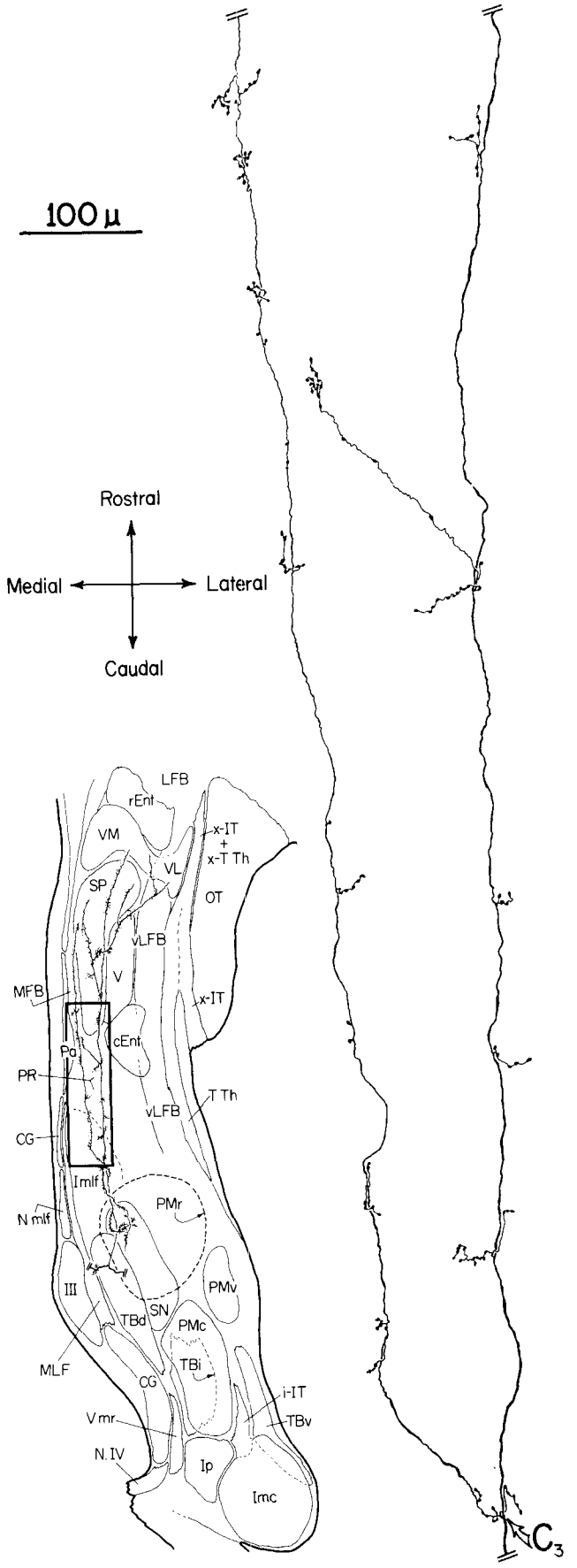

Continuing now with the anterograde results, just ventral and caudal to the decussating SC axons, the TBv(med) begins giving off medially directed collaterals again, this time into the small-celled ventrolateral segment of reticularis superioris lateralis (Fig. 2F,G). At first, these collaterals encroach only slightly on the dorsomedially contiguous TBi terminal field in the dorsomedial segment of reticularis superioris lateralis, but by the time the rostral pole of the trigeminal complex is reached, there is an extensive overlap in the terminal fields of these two tracts. The TBv(sm), by contrast, continues to generate only a sheet-like terminal zone embedded within the pathway. As the tracts pass under reticularis medius, the TBv(med) collaterals take a more dorsal course and some extend dorsolaterally by the level of the abducens nucleus. Caudal to the facial nucleus, TBv(med) collaterals travel laterally. The shift results from the more medial placement of the parent axons at caudal levels in the brainstem. Substantial overlap with the TBi terminal field continues. The sheet-like terminal zone produced by TBv(sm) appears to end in the medulla, but a few by now thin TBv(med) axons still emit collaterals at the level of the hypoglossal nucleus. Staining in these axons fades at the obex. *To summarize*, TBv(med) generates a continuous terminal field throughout the ventrolateral aspect of the reticular core while TBv(sm) generates a more restricted sheet on the ventral surface of the brainstem.

It seems unlikely that more than a few axons in the body of TBv were retrogradely filled for several reasons. First, although there is a sparse spinotectal projection (Künzle and Woodson, '82), it is contralateral and it decussates rostral to the obex. Caudal reticulotectal or trigeminotectal projections were also very sparse in the present material. However, one possibility cannot be ruled out. In the garter snake (Dacey, '82), a tectal-projecting nucleus just caudal to the obex and dorsal to the spinal canal gives off very large axons that enter the TBv in that animal. In the pond turtle, several very large axons (8 μm) were seen in the TBv(med) with large injections, but these faded without thinning at medullary levels.

Morphology of tectoreticular axons

The large injection just described filled many axons, making serial reconstruction of tectoreticular axons in each pathway impractical. By contrast, small injections filled only a few efferent axons in a given pathway, permitting single axons to be followed through serial sections. The following description is based on the substantially complete serial reconstruction of 19 TBd axons, 23 TBi axons, and 16

Fig. 10. Continuation of the main rostral branch shown in Figure 9. Another secondary collateral is given off at C_3 but unlike the collaterals at C_1 and C_2, C_3 travels rostrally along with the parent trunk. Both C and C_3 give off small clumps of boutons at regular intervals. These branches pass just lateral to the magnocellular spinal-projecting neurons in the interstitial nucleus of the medial longitudinal fasciculus (Imlf). The rectangle in the inset indicates the position of this reconstruction.

Fig. 11. Continuation of the rostral branches shown in Figures 9 and 10. The fourth and fifth secondary collaterals arise at C_4 and C_5. At C_5, the main branch makes a sharp turn to the right. Similar abrupt turns occurred in the main rostral branches of most TBd neurons once they were in the suprapeduncular nucleus (SP) although sometimes the turns were directed medially. The distal ends of these collaterals were rather lightly stained and it is possible that some may have penetrated the optic tract. The rectangle in the inset indicates the position of this reconstruction.

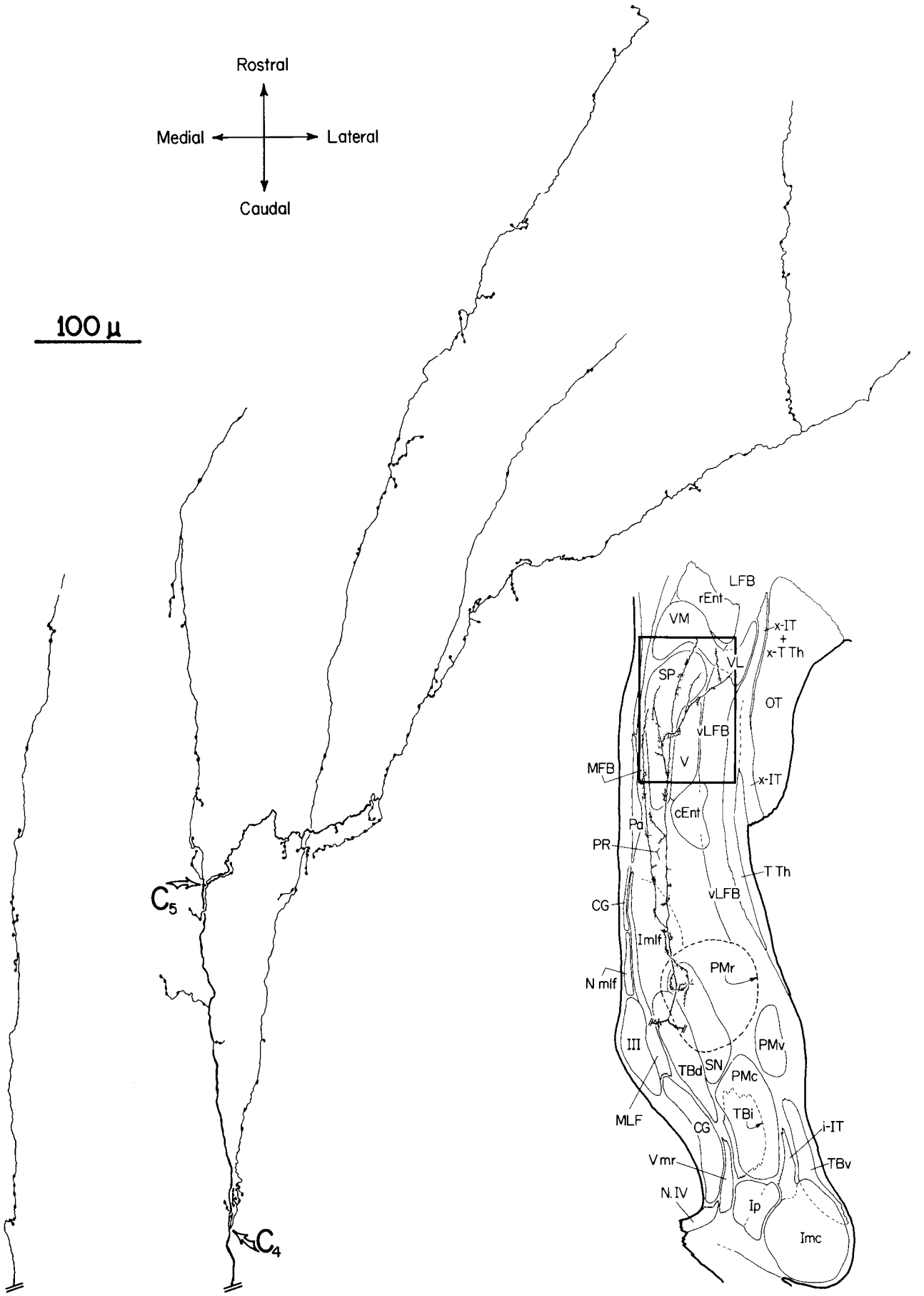
Rostral
Medial
Lateral
Caudal
100 µ
C5
C4
LFB
rEnt
VM
x-IT
+
x-T Th
VL
SP
OT
vLFB
V
MFB
x-IT
cEnt
Pa
PR
T Th
vLFB
CG
Imlf
PMr
N mlf
III
PMv
TBd
SN
PMc
MLF
TBi
CG
i-IT
Vmr
TBv
N. IV
Ip
Imc

Figure 11

TBv axons. Many more of each type were examined locally, or were partially reconstructed to determine typical patterns of branching.

Dorsal tectobulbar axons (TBd axons). Figure 5 is a summary of the branching pattern of TBd axons. These axons typically had three major parts: (1) rostrally directed branches in nucleus profundus mesencephali rostralis, (2) a robust, rostrally directed branch to the interstitial nucleus of the medial longitudinal fasciculus and the suprapeduncular nucleus, and (3) a caudally directed trunk that crosses the midline to run in the predorsal bundle.

Collaterals in profundus mesencephali rostralis (PMr). Rostrally directed collaterals to profundus mesencephali are schematically indicated in Figure 5A. The dorsoventral extent of these arbors is best seen in transverse reconstruction. Figure 6 is a partial reconstruction from six transverse sections of the ipsilateral collaterals of a TBd(lg) axon. Only the proximal portions of these branches are shown for clarity. Collaterals A and B were traced rostrally into profundus mesecephali rostralis as they branched. The stars indicate where these branches exit the front face of the most rostral section. Clearly, the branches span most of the dorsoventral extent of the nucleus. Boutons are not illustrated (most were rostral to this reconstruction) but arose from the main branches in small clusters throughout the volume of profundus mesencephali rostralis. One unusual branch of collateral B travels ventrally out of the nucleus to terminate in the interstitial nucleus of the medial longitudinal fasciculus. Continuing ventrally along the main trunk, collateral C is the thick rostrally directed branch that eventually terminates in the suprapeduncular nucleus. In this example, a proximal branch of collateral C almost penetrates the oculomotor nucleus. However, there was no collateral near the ventral aspect of the oculomotor nucleus from this axon like the ones seen on other TBd axons.

A different perspective is afforded by Figures 7–15, which comprise a complete reconstruction of a large caliber TBd axon and all its labeled collaterals, assembled from twenty-one 110 μm serial *horizontal* sections. The reconstructed TBd axon was traced out of the anterior of two small injection sites shown in Figure 4B. Each site emits a thin bundle of ventromedially directed TBd and TBi axons visible several sections ventrally in Figure 4A. The two bundles converge rostrocaudally before they leave the tectum. No collaterals were seen on TBd axons within the tectum.

After leaving the tectum, the main TBd trunk emits two rostrally directed collaterals (A and B) into profundus mesencephali rostralis (Fig. 7). Collateral A apparently becomes myelinated and then branches into three myelinated trunks that emit thin strings of boutons at intervals. The myelinated trunks themselves eventually thin out and begin to show boutons en passage after traveling about 500 μm (Fig. 4C). Collateral B is not myelinated. The main branches of collaterals A and B span almost the entire dorsoventral extent of profundus mesencephali rostralis (500 μm), penetrating variable distances into it in a rostromedial direction (i.e., along the rostrocaudal axis) before making 90° bends to run rostrolaterally along the dendrites of profundus mesencephali rostralis cells, which are confined mostly to planes approximately perpendicular to the rostrocaudal axis of the brainstem.

Boutons from anterogradely labeled TBd collaterals could often be observed contacting retrogradely labeled dendrites and somata in profundus mesencephali rostralis, in a manner suggestive of synapses. For example, the TBd collateral in Figure 8 (high-magnification view of boxed regions in Fig. 7) makes 14 apparent contacts on the proximal dendrites of a retrogradely filled profundus mesencephali cell and nine more on one of its distal dendrites. Collateral A also made a lesser number of apparent contacts with the dendrites (stippled shafts in Fig. 7) of five other back-labeled cells in the nucleus and the labeled soma of another. Figure 4D is a photomicrograph of apparent contacts from a TBd axon onto a profundus mesencephali rostralis neuron from a different case. Although the majority of the boutons supported by collaterals A and B are confined to profundus mesencephli rostralis, a few collaterals stray laterally into the tectothalamic tract (TTh), another meanders rostrally into the pretectum, and a few enter the central gray.

Main rostral collateral. In Figure 5B, the first branches have been omitted and the thick rostral branch that arises between the medial longitudinal fasciculus and the substantia nigra is schematically indicated in its long course under profundus mesencephali rostralis, through the interstitial nucleus of the medial longitudinal fasciculus, and finally into the suprapeduncular nucleus. The main rostral collateral in the horizontal reconstruction in Figure 7 is collateral C; it arises as the main trunk passes the oculomotor nucleus. This collateral is illustrated in detail in Figures 9–11. All TBd axons examined had a robust collateral at this level. These collaterals are as thick as 3 μm on TBd(lg) axons and 1 μm on TBd(sm) axons. As collateral C travels rostral and ventral to profundus mesencephali rostralis (Fig. 9), it gives off secondary collaterals (C_1 and C_2) which course dorsally for 500 to 700 μm, whereupon they arborize into fine branches that overlap those from collaterals A and B. Moving rostrally (Fig. 10), collateral C passes lateral to the large cells in the interstitial nucleus of the medial longitudinal fasciculus (Imlf). Another secondary collateral (C_3) arises, but unlike C_1 and C_2, travels forward, parallel to C. C and C_3 give off short strings of five to 15 boutons into the nearby tegmentum at regular intervals. They continue rostrally into the diencephalon where they enter the suprapeduncular nucleus (SP). At this point (Fig. 11), the secondary collaterals (C_4 and C_5) proceed laterally and probably end near the optic tract. The main collateral C, by contrast, makes an almost 90° lateral bend at this level (at C_5). Similar bends appeared in most collaterals of this type, as if they had suddenly run into invisible barriers. Occasionally, the collaterals turned medially into nucleus reuniens (Re). As in profundus mesencephali rostralis and the interstitial nucleus of the medial longitudinal fasciculus, moderate-sized clusters of boutons are distributed throughout the volume of the suprapeduncular nucleus.

Crossed collaterals. The morphology of the contralateral branches will be illustrated by two examples. The first

Fig. 12. Reconstruction from twelve horizontal sections of the contralateral course (through the predorsal bundle) of a dorsal pathway (TBd) axon. The ipsilateral collaterals of this axon were illustrated in Figures 7 and 9–11. The axon is plotted onto a horizontal reconstruction of a turtle brainstem made from alternate serial transverse sections. This axon emitted collaterals at regular intervals. Most of the thousand or so boutons supported by this axon are located in the medial half of the reticular formation. A few branches enter the raphe caudally. The axon was not completely filled past the level of the trigeminal motor nucleus. The rectangular regions in the inset labeled A–C are illustrated at a greater magnification in Figures 13–15.

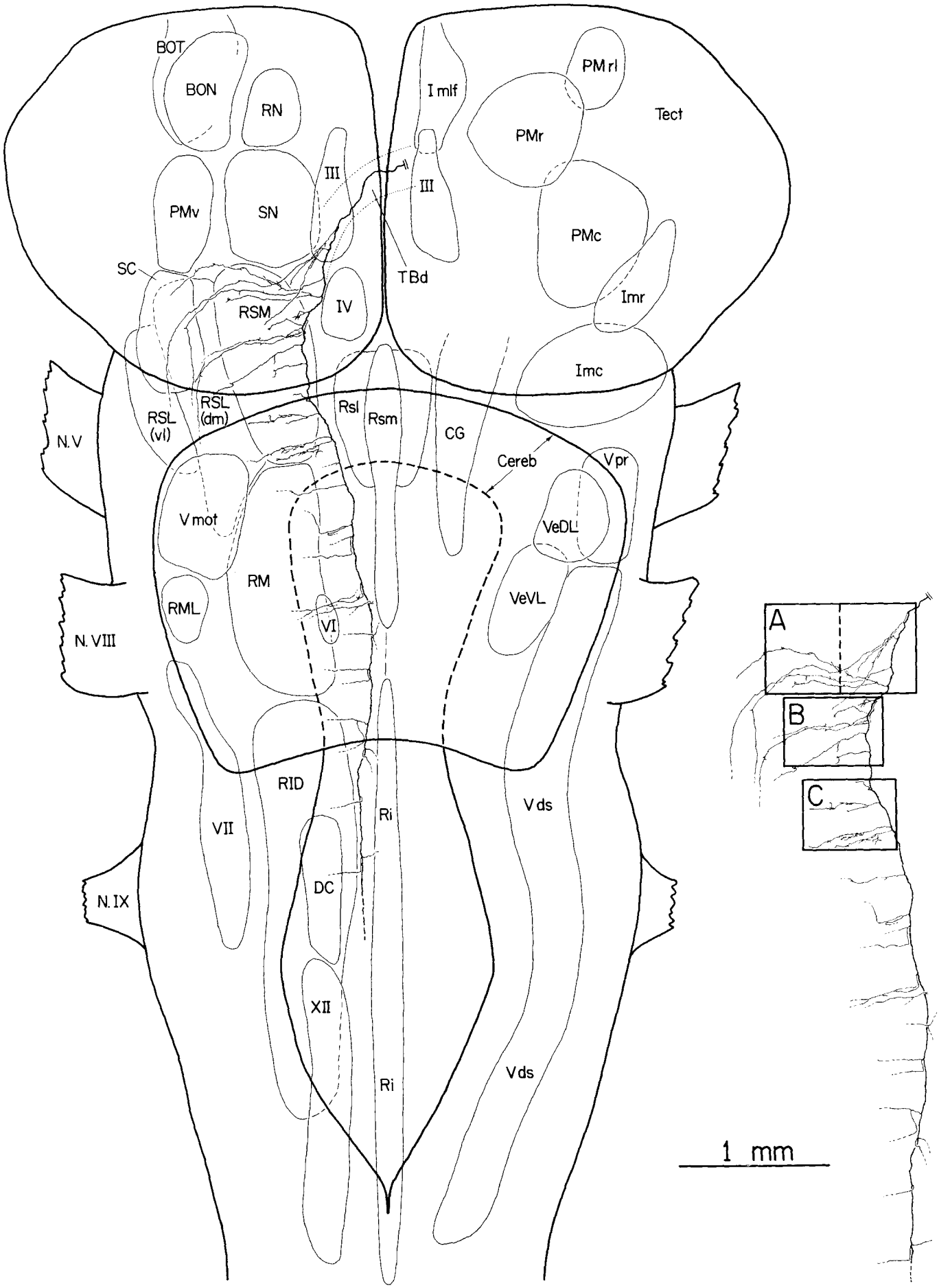
BOT
BON
RN
III
PMv
SN
SC
RSM
IV
RSL (vl)
RSL (dm)
N.V
Rsl
Rsm
CG
Cereb
Vpr
V mot
RM
RML
VI
N. VIII
RID
VII
N. IX
DC
XII
Ri
Vds
I mlf
III
TBd
PMrl
PMr
Tect
PMc
Imr
Imc
VeDL
VeVL
A
B
C
1 mm

Figure 12

Fig. 13. High-magnification view of region A of the dorsal pathway axon illustrated in Figure 12. The first contralateral collaterals (E, F) travel near the main trunk for a while before turning laterally, and thus avoid entering the substantia nigra. Subsequent branches course laterally from the start. Each contralateral collateral branches from a node in the thick (5–6 μm) myelinated main trunk with an initial diameter well under 1 μm. Portions of many collaterals thicken (up to 2 μm) and apparently myelinate (e.g., the initial 150 μm of collateral G). Small clumps of five to 20 boutons arise from unmyelinated preterminal strands. These clumps are distributed throughout the medial reticular formation. The inset shows one of the horizontal sections used to reconstruct this region of the axon and the rectangle indicates the location of the high-magnification view. Far laterally (outside the rectangle), collaterals thin to less than 1 μm and begin to wander caudally, giving rise to a few additional boutons in the small-celled nucleus (SC) ventral to Imc. In this and the succeeding high-power views, boutons have been drawn about twice their actual size to make their location apparent.

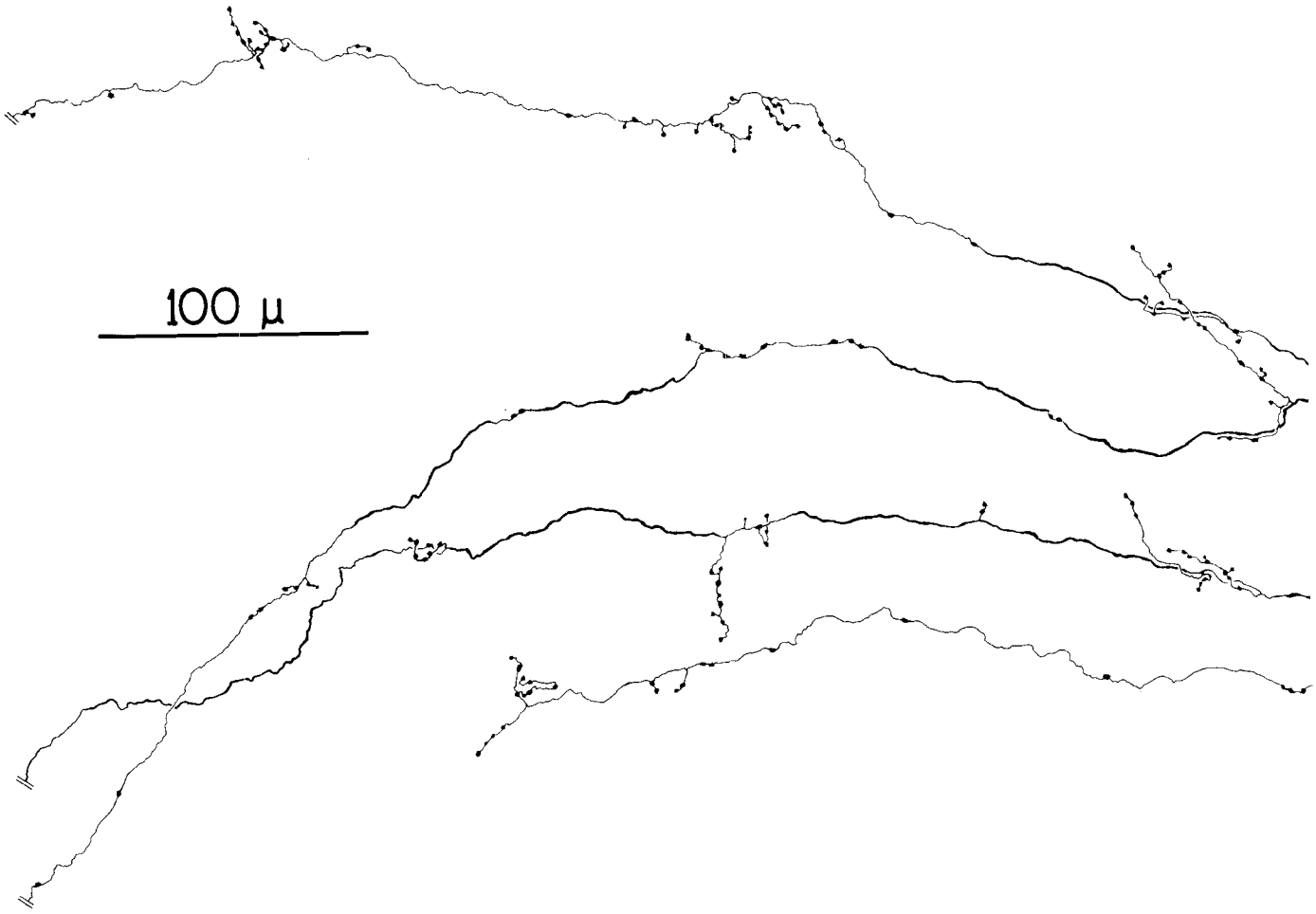

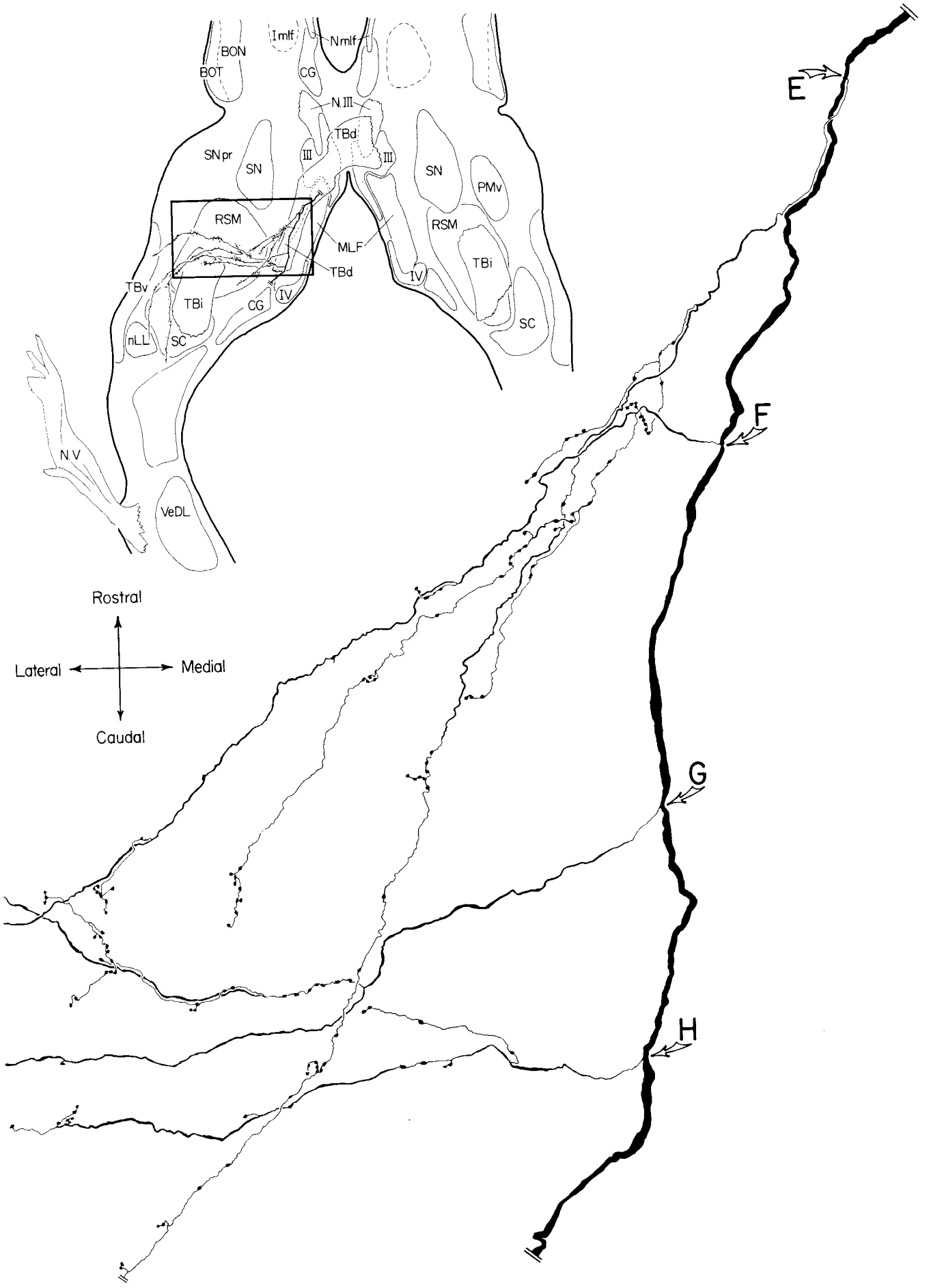
Imlf
Nmlf
BON
BOT
CG
N.III
TBd
III
SNpr
SN
SN
PMv
RSM
RSM
MLF
TBd
IV
TBi
TBv
TBi
CG
IV
nLL
SC
SC
N.V
VeDL
Rostral
Lateral
Medial
Caudal
E
F
G
H

Figure 13B

is the same axon shown in Figures 7–11. Its main trunk continues toward the midline after giving rise to the rostrally directed branches and emits a collateral (D in Fig. 9) ventral to the oculomotor complex that gives off a handful of varicosities just outside the medial longitudinal fasciculus and the oculomotor complex. A few other TBd axons did not have a collateral at this point, but such collaterals were identified in examples of both TBd(lg) and TBd(sm) axons. Figure 12 is a reconstruction of the contralateral course of the axon plotted to scale on a horizontal reconstruction from serial transverse sections. Figures 13–15 are higher-power views of the regions labeled A–C in Figure 12. It is clear that the axon was not completely filled caudally because boutons were not visible past the abducens nucleus, and large caliber collaterals faded without thinning. However, filling was still good over 6 mm from the injection site, in region C (Fig. 15), while in region A, collaterals could be traced until they became extremely thin and began "meandering," bearing only occasional (but well-filled) boutons.

The main trunk of the axon runs caudally in the predorsal bundle, sweeping laterally around the bulge in the midline nuclei at this level before coursing along the midline in the caudal pons and medulla. Contralateral collaterals arise regularly at intervals of 100–150 μm in the pons. The spacing between collaterals seems wider caudally, but it is possible that some were not filled. They have initial diameters under 1 μm and are nearly invisible for the first 10 or 20 μm. Many thicken and probably become myelinated after these initial constrictions. The first contralateral collaterals (E, F in Fig. 13) travel caudally for a considerable distance before turning into the reticular formation, thus avoiding the substantia nigra (SN) and the adjacent PMv (Fig. 12). Subsequent collaterals extend from the main trunk at almost right angles (Figs. 14, 15), generating a continuous terminal field throughout the reticular core. Clusters or short strings of five to 20 boutons are commonly seen. Some collaterals extend laterally up to 1 mm, entering the terminal field of the intermediate pathway, and a few travel up into the small-celled nucleus and terminate sparsely there. However, the density of boutons is much higher in the medial half of the reticular core. Thus, the terminal zone of the predorsal part of a single TBd neuron occupies, as was the case with its ipsilateral branches, virtually the same region as does the total projection.

A portion of a second TBd axon in the predorsal bundle is illustrated in Figure 16. This axon ran in the small caliber component of the TBd. It was traced out of a more caudal tectal site than the TBd(lg) fiber above, and gave off two ipsilateral, rostrally directed branches into profundus mesencephali rostralis, a long rostral branch to the suprapeduncular nucleus, and a fine twig just under the oculomotor nucleus before crossing to run in the small caliber part of the predorsal bundle. It is also similar to the previous TBd example in the caudal course of its initial contralateral collaterals, in the tendency for branches to occasionally penetrate the TBi field, and in the clumpy distribution of boutons. One difference is that there are about three times as many boutons situated within 200 μm of the trochlear nucleus. A second is that the axon also has a *contralateral* branch to the suprapeduncular nucleus arising from collateral D. It initially follows the surrounding branches caudally before making a 180° turn and traveling upward to enter the interstitial nucleus of the medial longitudinal fasciculus, and eventually the suprapeduncular nucleus. Thus, some TBd axons project to the suprapeduncular nucleus bilaterally. The more common pattern by far, however, is an ipsilateral-only connection.

Intermediate tectobulbar axons (TBi). An example of a TBi axon is illustrated in Figures 17–25. It was reconstructed from twenty-one 110 μm serial horizontal sections. Figure 17 is a low-power reconstruction of most of this axon plotted to scale onto the same topographical reconstruction used in Figure 12. This axon was traced into injection site A in Figure 27. Figures 18, 19, and 22–25 are high-power views of the regions labeled B,A, C–F in Figure 17. Figures 20 and 21 are high-power views of the end of the thick rostral collateral; these regions are located beyond the rostral edge of the low-power reconstruction in Figure 17. The main collaterals are lettered sequentially in the high-power views.

Figure 18 illustrates the first collaterals visible after the myelinated, 2.5 μm diameter main trunk emerges from the injection site. The main trunk travels (almost perpendicular to the plane of section) through profundus mesencephali caudalis (PMc). The branches labeled A–D distribute strings of 25–75 boutons to the medial third of the nucleus. Some collaterals also reach the laminated and central nuclei of the torus semicircularis (Torl and Torc) and the central gray (CG). Many partially reconstructed TBi axons showed a similar overall pattern, distributing collaterals to only a part of profundus mesencephali caudalis. A point-to-point topography, however, was not evident. In contrast to the common observation of TBd boutons in apparent contact with back-labeled profundus mesencephali rostralis cells, TBi boutons were not observed to contact back-labeled profundus mesencephali caudalis cells; in a number of cases, labeled cells in the caudal nucleus were seen lateral to the TBi terminal field. Profundus mesencephali caudalis cells also had less extensive dendritic fields and smaller somata than profundus mesencephali rostralis cells.

The rostrally directed collateral at B is unique in that it is by far the thickest. It branches from the main trunk with a diameter of over 1 μm and then expands to almost 2 μm, apparently becoming myelinated for most of its course. By contrast, the other collaterals are constricted to well under 1 μm in diameter at their point of origin and are not myelinated. The majority of TBi axons had one robust, rostrally directed branch among the first several collaterals. These branches avoided profundus mesencephali rostralis, either passing medial or ventral to it. In this example, collateral B runs between the medial edge of that nucleus and the central gray (Figs. 18, 19), pierces the central gray at the posterior commissure, and courses rostrally through the neuropile between the central gray and the ependyma for almost a millimeter (Fig. 20), until it passes by the dorsal

Fig. 14. High-magnification view of region B of the dorsal pathway axon illustrated in Figure 12. As in Figure 13, collaterals arise at regular intervals and distribute small clumps of boutons to many parts of the medial reticular formation. A slightly increased density of termination is evident near the origins of collaterals I and J. The axon is passing beneath the caudal pole of the trochlear nucleus at this level (see Fig. 12). The main trunk begins to curve back toward the midline after traveling around the bulge in midline structures that is created by the superior raphe nuclei and the interpeduncular nuclei (Rsl, Rsm, Ipd, and Ipv). The location of the high-magnification view is shown in the inset. Collaterals that reached the lateral reticular formation (RSL, lateral to the rectangle in the inset) became very thin and gave off only four more boutons.

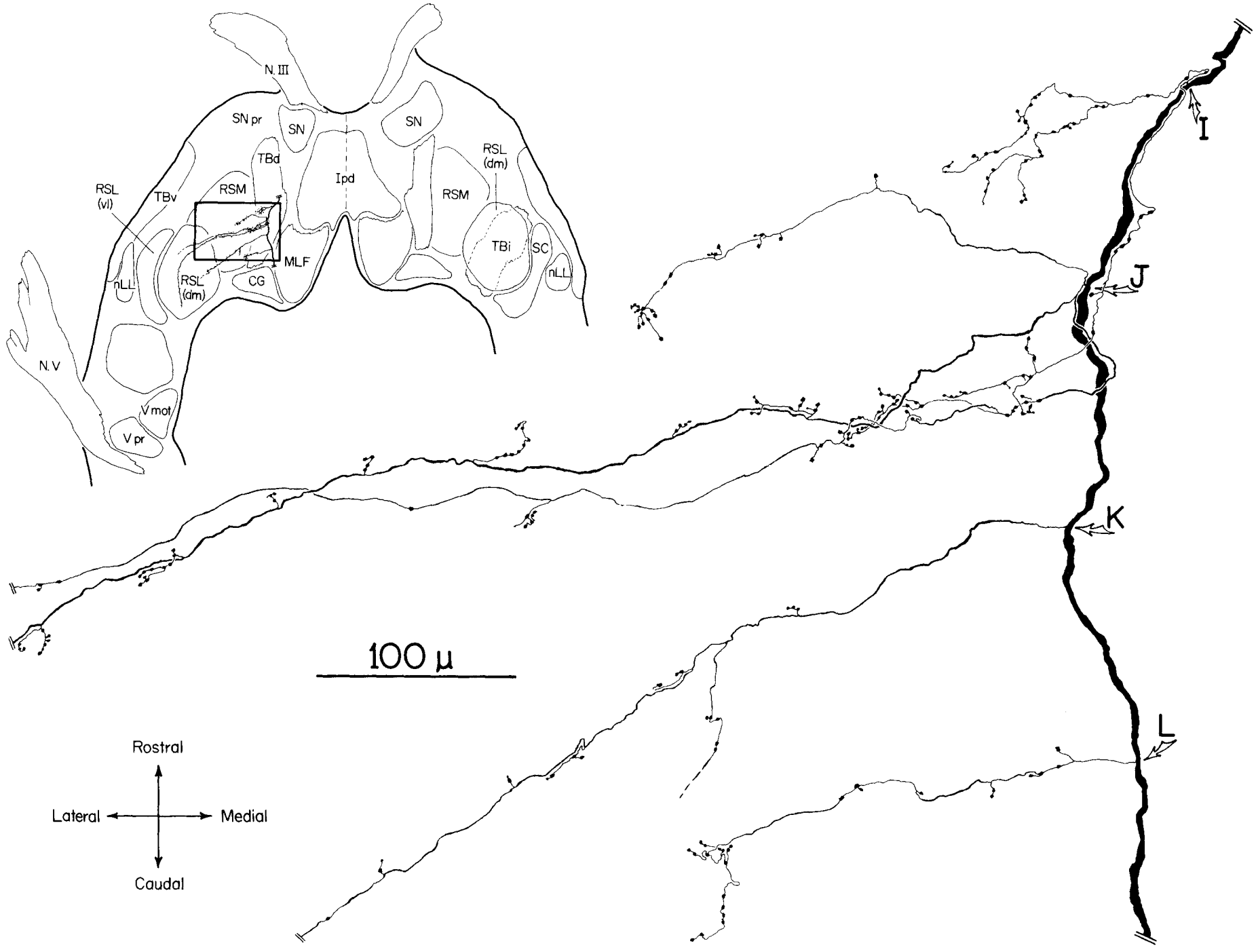
N. III
SN pr
SN
SN
TBd
Ipd
RSL (dm)
RSL (vl)
TBv
RSM
RSM
TBi
SC
nLL
MLF
RSL (dm)
CG
nLL
N. V
V mot
V pr
I
J
K
L
100 µ
Rostral
Lateral
Medial
Caudal

Figure 14

edge of the nucleus of the medial longitudinal fasciculus (Nmlf, Fig. 21). Just rostral to that nucleus, the collateral penetrates back through the pretectal central gray, continues rostrally, and then abruptly turns into the lateral hypothalamic area (Fig. 21) where thin unmyelinated stretches begin to appear in the main collateral trunk. It continues laterally until it enters the ventral peduncle of the lateral forebrain bundle where it turns and runs *caudally* for several millimeters, after which it was lost. The main myelinated trunk of collateral B gives off short branching strings of ten to 75 boutons at intervals of approximately 100 μm throughout most of its course. No strings are emitted for a 400 μm stretch as the collateral passes through the bundle of ventrally directed TBd axons (Fig. 19), and only a few boutons arise in the lateral hypothalamic area and even fewer in the long meandering path back through the lateral forebrain bundle.

Figures 22–25 (regions C–F in Fig. 17) illustrate selected portions of the main caudal trunk and its collaterals. The axon was densely filled to the midpoint of the facial motor nucleus, which is about 7 mm from the injection site. The main trunk turns laterally (Figs. 22, 23) as it passes the bulge in the midline nuclei near the pons-midbrain junction. It then recurves medially (Figs. 24, 25), but remains in the lateral half of the reticular core. Collaterals are emitted at approximately 100 μm intervals until the main trunk passes well into reticularis inferioris dorsalis, where branches arise less frequently. As with TBd collaterals, TBi collaterals are given off from the main myelinated trunk with a diameter well under 1 μm, and often travel a short distance closely apposed to the main trunk before turning laterally. In this TBi axon, most collaterals course medially but, collaterals sometimes travelled laterally in other axons where the main trunk was located a little closer to the midline (e.g., photomicrograph in Fig. 26A). Each collateral bears 25–75 synaptic boutons, often arranged into small clumps of five to 20 boutons. The majority of the terminals are in the lateral reticular formation—the dorsomedial segment of reticularis superioris lateralis and the lateral half of reticularis medius and reticularis inferioris. A number of collaterals penetrated the medial TBd terminal field (Figs. 23–25) but deposited relatively few terminals there. Collateral G entered the small-celled nucleus and gave off a small branch bearing very fine boutons (Fig. 22—low-power drawing). A similar overall pattern of arborization in the lateral half of the reticular core could be distinguished in other TBi axons. In some axons, medially directed collaterals reached the caudal central gray at the level of the trigeminal motor nucleus. Thus, as with TBd axons, the terminal zone of a single TBi axon occupies almost the same region as the total projection. The axon in Figures 17–25 emitted a little over 2,700 boutons in its visible course. Perhaps 200–500 additional boutons might have been missed by light filling far caudally and by conservative reconstruction practices.

Ventral tectobulbar axons (TBv axons). Single ventral pathway axons, like intermediate and dorsal pathway axons, have extensive brainstem distributions. However, TBv axons apparently do not have thick rostral collaterals, and their caudal trunks branch less extensively. Furthermore, TBv axons often have intratectal collaterals and, probably, commissural branches to the contralateral tectum (Sereno and Ulinski, '85) both of which were never seen in TBd and TBi axons. It was difficult to get a complete picture of TBv axonal morphology at the single-cell level because even small injections resulted in a formidable tangle of afferents and other efferents near the point where TBv axons leave the tectum. For the small caliber component of the TBv, this was remedied by reconstructing axons that were retrogradely labeled from the tegmentum (see Materials and Methods of the following paper).

Small caliber TBv axons. Figure 27 is a serial reconstruction of the intratectal course of a retrogradely labeled TBv(sm) axon and a schematic diagram of its course through the brainstem. The 1 μm diameter axon arises from the descending radial dendrite of a small bitufted cell in the stratum fibrosum et griseum superficiale (SFGS) and runs just below the deepest retinal terminal zone, between layers 7 and 8 of Ramón (1896). Collaterals bearing many *boutons en passage* arise every 100–200 μm and descend through the central gray (SGC) and white (SAC) layers, sometimes entering the deep periventricular gray (SGP). Collaterals strictly avoided the retinal recipient stratum fibrosum et griseum superficiale in this and other examples. This collateral field ends abruptly as the main axon trunk leaves the tectum and enters the rostral magnocellular isthmi (Imr). It passes all the way through the almond-shaped mass of fibers and terminals that engulfs the nucleus (only lightly labeled by this *tegmental* injection) without generating any collaterals. Soon after passing out of rostral magnocellular isthmi, the axon makes a downward bend into the fine caliber component of the ventral pathway just ventrolateral the caudal magnocellular nucleus isthmi (Imc). Here, several long collaterals are given off into the dorsal half of the small-celled nucleus just under caudal magnocellular isthmi. The axon then runs along the ventrolateral surface of the brainstem emitting short collaterals into the neuropile there, until it was lost entering the injection site. Several other small bitufted cells in the stratum fibrosum et griseum superficiale that were reconstructed also had axons with intratectal collaterals, a lack of collaterals as the main trunk passed through rostral magnocellular isthmi, long collaterals to the small-celled nucleus, and short collaterals in the neuropile at the ventrolateral surface of the brainstem. The source of the almond-shaped mass of fine terminals in rostral magnocellular nucleus isthmi (Fig. 2G) and of the dense field of fine terminals in the neuropile *lateral* to the small-celled nucleus (Fig. 2F) was not determined. A possible source is the population of small radial cells in the SGP that have the smallest caliber axons of any tectobulbar cells.

Medium caliber TBv axons. The following paper suggests, on the basis of retrogradely labeled material, that TBv(med) axons also tend to have intratectal collaterals. In several cases, putative TBv(med) cells had an axon branch that crossed in the tectal commissure (e.g., Fig. 10 from Sereno and Ulinski, '85). After TBv(med) axons pass through the ipsilateral i-IT, it becomes possible to follow single axons through serial sections in anterogradely labeled material. These axons are the main source of collaterals to the small-celled nucleus. As the parent axon passes the lateral edge of the nucleus, two or three branches arise,

Fig. 15. High-magnification view of region C of the dorsal pathway axon illustrated in Figure 12. At this level (6–7 mm from the injection site) the HRP filling begins to lighten (e.g., see the lateral end of collateral O). The main trunk remains thick and could be followed for 3 more mm. It continued to give off collaterals at regular intervals but these were too lightly stained to distinguish boutons. The main trunk faded in the medullary reticular formation.

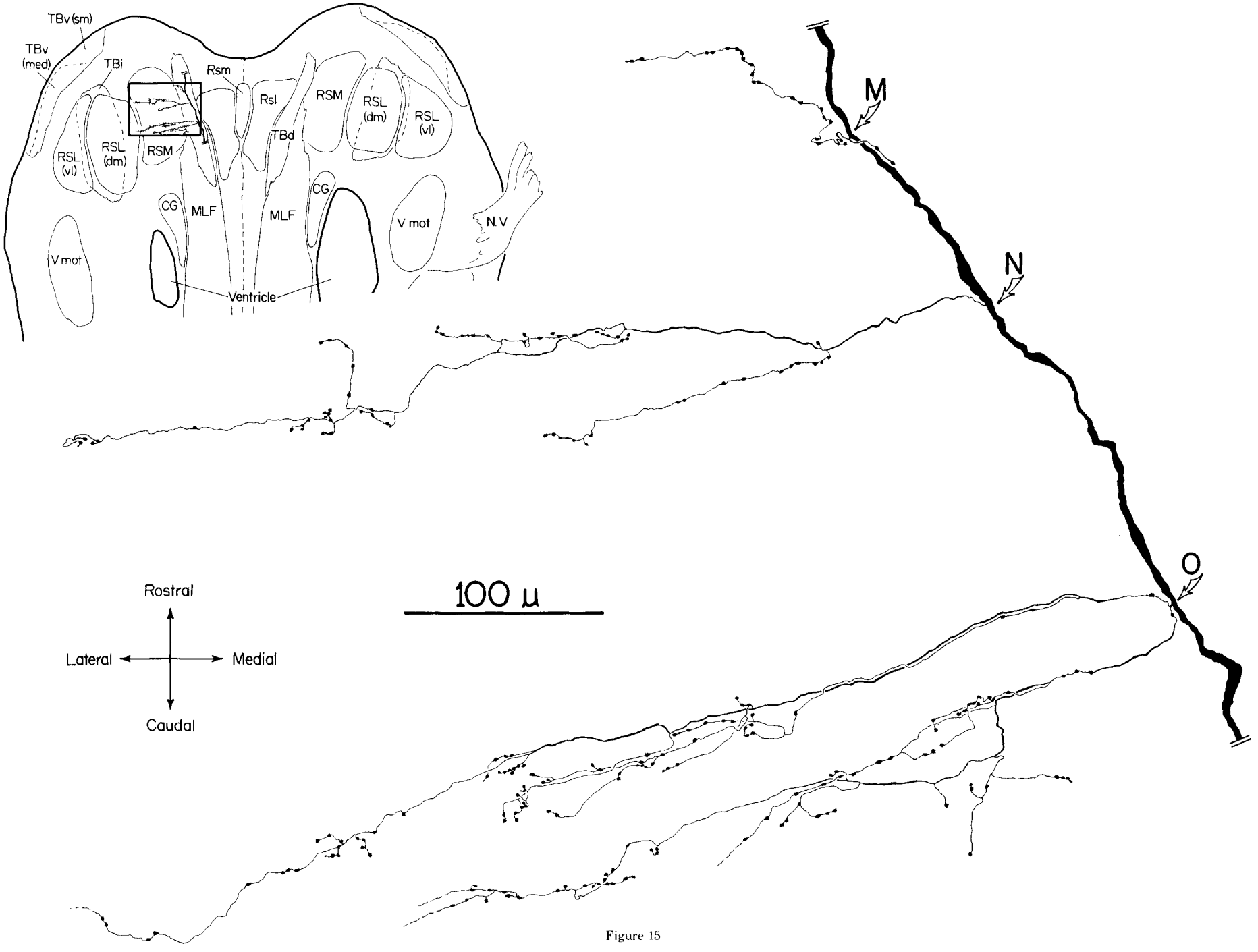
TBv (sm)
TBv (med)
TBi
Rsm
Rsl
RSM
RSL (dm)
RSL (vl)
TBd
RSL (vl)
RSL (dm)
RSM
CG
MLF
MLF
CG
V mot
N.V
V mot
Ventricle
M
N
O
100 μ
Rostral
Lateral
Medial
Caudal

Figure 15

subdivide, and give rise to about 30–100 boutons distributed across a significant portion of its dorsal segment. Almost all TBv(med) axons had branches to the small-celled nucleus. Caudal to it, the main trunks of the axons travel ventrally for about a millimeter until they reach the ventrolateral segment of the reticularis superioris lateralis (RSL(vl)), where they emit several collaterals (Fig. 28). These branches usually avoid the more medially located TBi terminal field in the dorsomedial segment of reticularis superioris lateralis. Further caudally, in reticularis medius and reticularis inferioris dorsalis, however, there is significant overlap between the TBi and TBv(med) terminal fields. The morphology of those TBv(med) collaterals is similar to the ones shown in Figure 28. Compared to TBi axons, TBv(med) axons branch less frequently in the tegmentum and could often be followed for a millimeter at a time without a branch. No topographic pattern was discernible but the sample of reconstructed axons was small. A few TBd(med) axons were still visible at the level of the hypoglossal nucleus.

Topography of the TBi projection

There was no obvious topographic pattern in the tectoreticular projections as the location of the injection site in the tectum was varied. However, cases with two injections at different loci sometimes resulted in separated clumps of main axon trunks in the pontine reticular formation. Furthermore, the TBi "tract" spans up to 750 μm dorsoventrally in contrast to the more localized (and hence recognizable) predorsal bundle (TBd axons). Given that the majority of the boutons arising from a TBi axon are found within 200 μm of the main trunk, and often in dorsoventrally flattened arrays, a crude dorsoventral and/or mediolateral mapping of tectal loci seemed possible. Also, given the low density of the projection, such a topography might have been overlooked with conventional plotting techniques. Therefore it was decided to examine the topography at the level of single axons. Figure 29 is a stereoscopic view of the main trunks of 17 TBi axons emerging from two punctate injection sites and coursing into the lateral pontine reticular formation. Two small HRP injections at A and B labeled eight (Nos. 1–8) and nine (Nos. 9–17) TBi axons, respectively, each of which was traced through 16 horizontal serial sections. The axons all entered the dorsomedial segment of reticularis superioris lateralis where they sorted into two distinct clumps. The caudal ends of axons 1, 4, 5, 7, 10–13, 16, and 17 are located in a flattened clump about 500 μm dorsal to axons 2, 3, 6, 8, 9, 14, and 15. Most axons remained with one clump throughout the dorsomedial segment of reticularis superioris lateralis; axon 8, by contrast, started out in the dorsal group but then made an abrupt jump to the ventral group that is visible at the middle of the figure. Each clump obviously contains a mixture of axons from the two injection sites, suggesting that there is no point-to-point topography at the level of small groups of axons. The axon previously illustrated in detail in Figures 17–25 is axon number 2 (circled); it emerged from site A and ended up in the ventral clump. All 17 axons were between 1.5 and 2.5 μm in diameter. For clarity, however, the axons from injection site A have been drawn thicker to distinguish them from site B axons. Thirteen of the 17 axons shown had one thick, rostrally directed collateral that arose as the axons turned caudally; these are not drawn in Figure 29.

DISCUSSION

These results indicate that tectoreticular projections in turtles comprise three main pathways containing axons of several sizes. The pathways are schematically illustrated in Figure 30. Single tectoreticular axons in each pathway terminate sparsely and non-topographically in a variety of reticular structures throughout the brainstem. One axon typically supports several thousand boutons. Comparable numbers of boutons are supported by single axons in topographically organized pathways like the ipsilateral isthmotectal pathway (from caudal magnocellular isthmi) where each axon gives rise to a dense, spatially restricted terminal thicket whose location varies systematically with the map location of the neuron's dendritic field in the nucleus (Sereno, '83). The boutons of a tectoreticular axon, by contrast, are distributed throughout an immensely greater volume and are intermingled with boutons originating from tectobulbar neurons at many different, non-adjacent tectal loci. This discussion will consider some general features of the three pathways. Functional implications of the organization of the pathways will be discussed in the accompanying paper after the morphology of the parent cells has been established.

The *dorsal tectobulbar pathway* is constant across vertebrate classes. It has been characterized at the single-cell level in turtles, snakes (Dacey, '82), and cats (Grantyn and Grantyn, '82; Grantyn et al., '82). In all three animals, dorsal pathway axons lack intratectal collaterals and have ipsilateral branches into the rostral mesencephalic tegmentum and central gray, as well as a main rostral branch that reaches the ventral thalamus (via "medial tectothalamic tract" in Dacey, '82). In cats, this last branch arises at the level of the oculomotor nucleus and travels just lateral to the interstitial nucleus of Cajal (= interstitial nucleus of the medial longitudinal fasciculus in reptiles) to reach the rostral interstitial nucleus of the medial longitudinal fasciculus (see Buttner-Ennever and Buttner, '78) and the zona incerta (probably together equivalent to the reptilian SP). In turtles, visual and somatosensory responses have been recorded in the suprapeduncular nucleus, and visually driven activity there is almost completely abolished by ipsilateral tectal lesions (Belekhova, '79).

A similar pattern of ipsilateral branching can be inferred from anterograde tracer and degeneration experiments in a number of other animals. In monkeys, for example, Harting et al. ('80) showed a rostrally directed "fine caliber component" of the dorsal pathway arising just before the thick predorsal bundle axons decussate. These thinner axons travel lateral to the interstitial nucleus of Cajal to reach the rostral interstitial nucleus of the medial longitudinal fasciculus where some turn laterally into the zona incerta. In birds, Hunt and Künzle ('76, their Fig. 4B) demonstrated a rostrally directed fascicle arising from the dorsal tectobulbar pathway that eventually terminates in the ipsilateral nucleus subrotundus. In *Iguana*, Foster and Hall ('75, their Figs. 5, 6) showed a similar projection to the "ventromedial thalamic nucleus" while Ebbesson and Vanegas ('76) illustrate a "recurrent rostral bundle" leaving the dorsal pathway to enter the ventral thalamus in two teleost species.

The detailed pattern of contralateral branching is also uniform across vertebrates. For example, a second thick rostral collateral occasionally arises *after* the main trunk

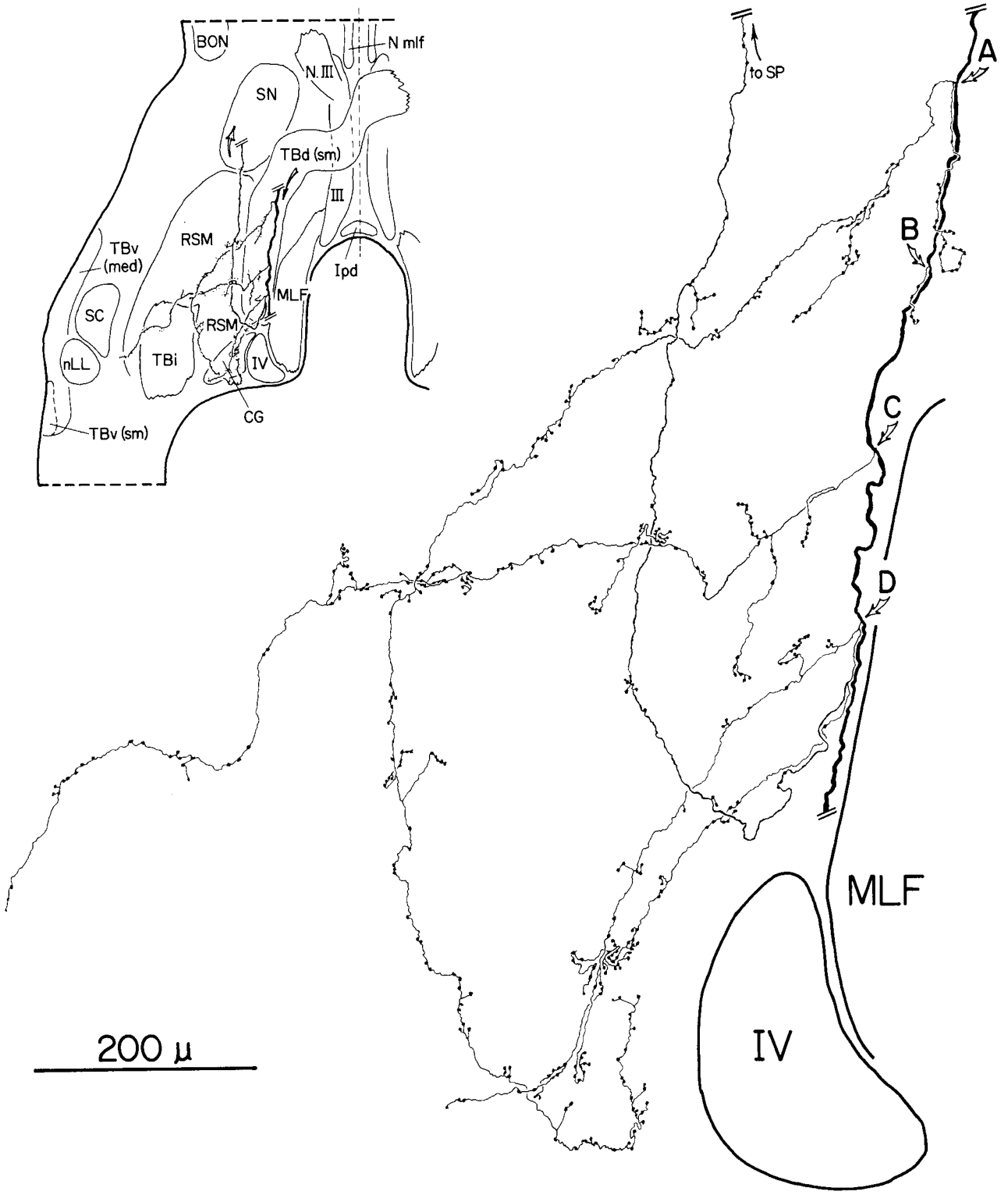

Fig. 16. Reconstruction of the first four contralateral branches of an axon in the small caliber component of the dorsal pathway, TBd(sm). As with large caliber dorsal pathway axons, this axon had ipsilateral collaterals (not shown) including branches to profundus mesencephali rostralis (PMr), a "main rostral collateral" eventually reaching the suprapeduncular nucleus (SP), and a small twig near the oculomotor nucleus. The first contralateral collaterals trend caudally. The main trunk (2 μm diameter) is myelinated as are some of the thicker collaterals (parts of collateral D). This axon has a *contralateral* branch to the suprapeduncular nucleus in addition to a more usual ipsilateral branch; it arises from collateral D, initially runs caudally, and then makes a 180° turn to run rostrally through the interstitial nucleus of the medial longitudinal fasciculus (Imlf), eventually reaching SP. This axon also has about three times as many boutons within 200 μm of the overlying trochlear nucleus as did the previous example in Figures 12–15 (for a similar-sized brain). Since the original drawing was reduced more in this illustration, boutons were drawn at about four times actual size to make them visible.

has decussated; such a collateral can reach the contralateral ventral thalamus in turtles (Fig. 16, collateral D) as well as in cats (collateral 3 in Fig. 3 of Grantyn et al., '82). Caudally, the extensive collaterals of dorsal pathway axons in cat, snake, and turtle apparently differ only in scale. Thus, a 5 μm diameter main trunk gives off branches every 150 μm in the turtle while a 9 μm predorsal axon in the cat emits approximately the same number of collaterals (over a course three times as long) at about 700 μm intervals. A few medially directed collaterals travel into or near the raphe just caudal to the abducens nucleus in cats and turtles. The paramedian terminal field of the predorsal bundle is present in all other vertebrates examined, the primary difference in bony fish and amphibians being that the parent axons are more ventrally placed (Rubinson, '68; Luiten, '81). A small caliber component of the dorsal pathway ventral to the large caliber component has not yet been recognized in animals besides turtles and snakes. However, it may have been mistaken for a terminal field in anterograde tracer studies. Small axons were not recovered after intracellular injections in the predorsal bundle (Grantyn and Grantyn, '82), but this could be due to a sampling problem.

The *intermediate tectobulbar pathway* is known at the single-cell level only in turtles and snakes where it can be aptly described as a more laterally terminating, ipsilateral version of the dorsal pathway. As with dorsal pathway axons, intermediate pathway axons have one main rostral collateral. However, these branches were not present in every case and their rostral course through the pretectal central gray near the nucleus of the medial longitudinal fasciculus was somewhat variable. Thus, the intermediate pathway axon illustrated by Dacey ('82) apparently lacked an identifiable main rostral branch, though these were present on other axons (personal observation). Harting et al. ('80) has demonstrated a deep tectal projection to the rostral central gray in monkeys. Nevertheless, given the variable course of these branches, it will be necessary to characterize axons in this pathway at the single cell level before more firm comparisons can be made.

The turtle and snake material is similar at caudal levels. In both animals, single intermediate pathway axons terminate first in the caudal mesencephalic tegmentum and then throughout the lateral reticular core, occasionally also giving off branches to the caudal central gray and the trigeminal complex. The intermediate pathway is especially well developed in cartilaginous fishes (Smeets, '81) but can be clearly distinguished in other reptiles (Foster and Hall, '75) and birds (Hunt and Kunzle, '76; labeled "ventral tectobulbar pathway") as well. Most who have worked on mammals have not explicitly distinguished intermediate and ventral pathways (e.g., Burne et al., '81; Harting and Huerta, '82). Nevertheless, the recent experiments of Holcombe and Hall ('81a,b) using restricted injections demonstrate that different sets of tectal neurons project to the ventrolateral pontine tegmentum on one hand, and the underlying dorsolateral pontine nuclei on the other. In squirrels, cats, and monkeys, the intermediate pathway emits a dense terminal field in the caudal part of the cuneiform nucleus before terminating more lightly in the lateral half of the pontine reticular core (Harting, '77; Holcombe and Hall, '81a; Harting and Huerta, '82).

The *ventral tectobulbar pathway* is the most variable, probably in part the result of its involvement with the pontine nuclei, which appear in birds and mammals (Clarke, '77; Brown-Gould, '80; Bangma and ten Donkelaar, '82). Single-cell information about this pathway, however, is only available in turtles and snakes, which themselves show significant differences. Turtle ventral pathway axons have intratectal and commissural collaterals that were not seen in snakes. Turtle axons then pass without branching through the rostral (non-topographic) nucleus isthmi (Imr) and collateralize in a small-celled nucleus ventral to the caudal (topographic) nucleus isthmi (Imc), rather than *in* the topographic nucleus isthmi itself as do snake axons. Finally, the turtle ventral pathway has a medium caliber component that emits collaterals partially overlapping the intermediate pathway terminal field in the caudal pons and medulla, in addition to the small caliber pathway terminating exclusively in the ventrolateral neuropile that is seen by itself in snakes. In birds, Hunt and Künzle ('76) have described a tectopontine pathway that appears similar to the ventral pathway. It passes through the non-topographic nucleus isthmi magnocellularis (probably equivalent to turtle Imr) and then passes just lateral to the topographic nucleus isthmi parvocellularis (probably equivalent to turtle Imc) before terminating non-topographically in the lateral pontine nucleus. Recently it has been suggested that the rat tectopontine projection is topographically organized (Burne et al., '81). Cats and primates, too, exhibit a complex tectopontine projection (Harting, '77; Harting and Huerta, '82). Since retrograde tracer experiments have uncovered no evidence of cerebellar projecting neurons in the reptilian ventral pons (Bangma and ten Donkelaar, '82), it appears that the ventral tectobulbar pathway has been secondarily recruited into a tecto-ponto-cerebellar circuit.

ACKNOWLEDGMENTS

I thank Dr. P.S. Ulinski and Dr. D.M. Dacey for advice and encouragement. This work was supported by PHS grant NS 12518 and an NSF predoctoral fellowship.

LITERATURE CITED

Abrahams, V.C., and P.K. Rose (1975a) The spinal course and distribution of fore and hind limb muscle afferent projections to the superior colliculus of the cat. J. Physiol. (Lond.) *247*:117–130.

Abrahams, V.C., and P.K. Rose (1975b) Projections of extraocular, neck muscle, and retinal afferents to superior colliculus in the cat: Their connections to cells of origin of the tectospinal tract. J. Neurophysiol. *38*:10–18.

Adams, J.C. (1977) Technical considerations on the use of horseradish peroxidase as a neuronal marker. Neuroscience *2*:141–145.

Adamük, E. (1870) Über die Innervation der Augenbewegungen. Zentrabl. Med. Wiss. *8*:65.

Akert, K. (1945) Der visuelle Greifreflex. Helv. Physiol. Acta. *7*:112–134.

Altman, J., and M.C. Carpenter (1961) Fiber projections of the superior colliculus in the cat. J. Comp. Neurol. *116*:157–178.

Balaban, C.D., and P.S. Ulinski (1981) Organization of thalamic afferents to anterior dorsal ventricular ridge in turtles. I. Projections of thalamic nuclei. J. Comp. Neurol. *200*:95–129.

Fig. 17. Reconstruction from twenty-one 110 μm serial horizontal sections of an intermediate pathway (TBi) axon. As with dorsal pathway axons, this axon has a myelinated main rostral branch, and it gives off collaterals bearing small clumps of boutons at many levels throughout the brainstem. The main differences are: (1) the great majority of the boutons are in the lateral half of the reticular core, and (2) the caudal trunk does not cross. This axon was densely filled to the midpoint of the facial motor nucleus but quite faint by the time it passed the hypoglossal nucleus. It had thinned considerably before fading completely. The rectangular regions in the inset labeled A–F are illustrated at greater magnification in the next figures in the order B, A, and the C–F.

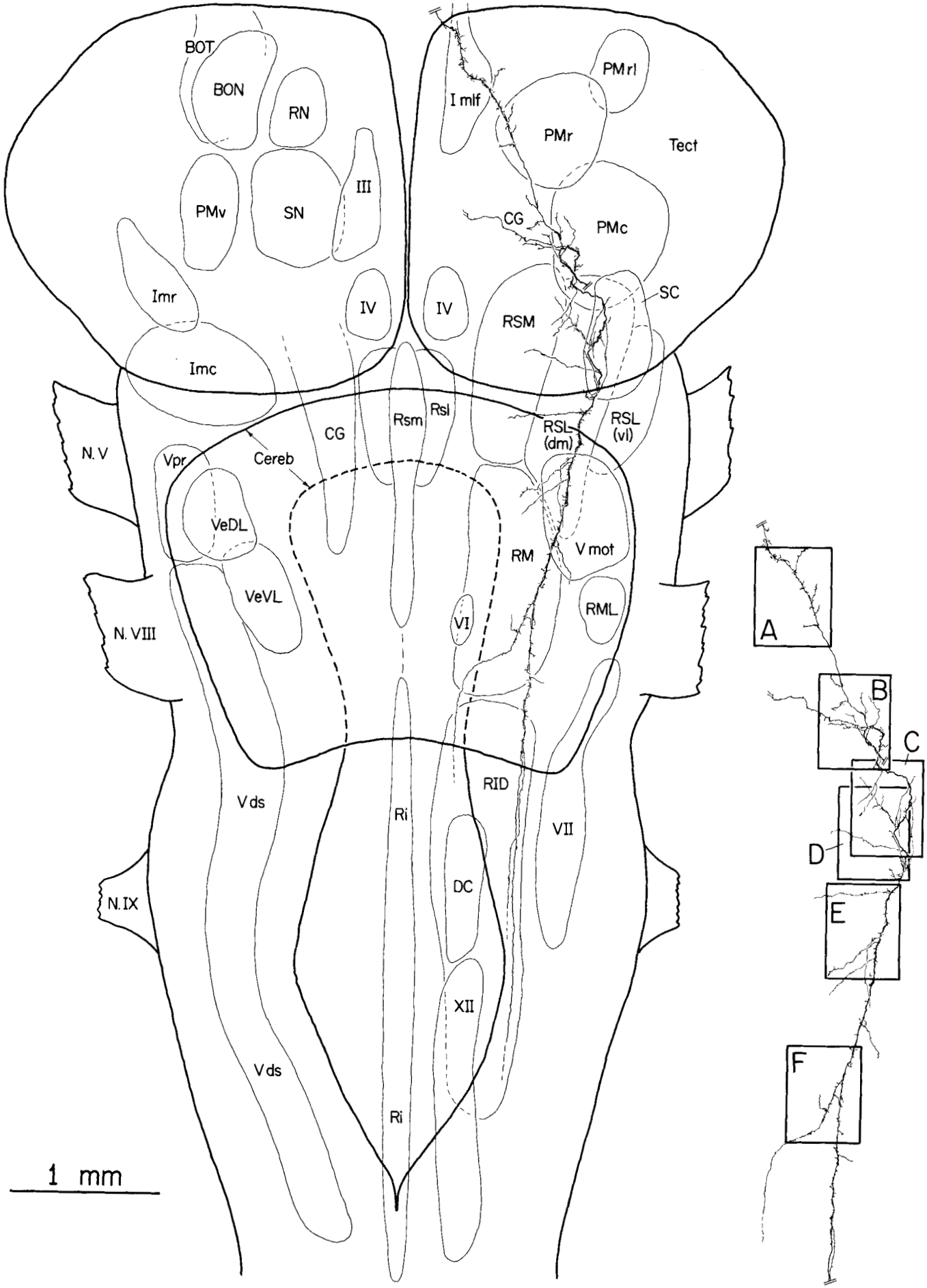
BOT
BON
RN
III
PMv
SN
Imr
Imc
IV
IV
I mlf
PMrl
PMr
Tect
CG
PMc
SC
RSM
N. V
Vpr
Cereb
CG
Rsm
Rsl
RSL (dm)
RSL (vl)
VeDL
VeVL
RM
V mot
RML
N. VIII
VI
Vds
Ri
RID
VII
DC
N. IX
XII
Vds
Ri
1 mm
A
B
C
D
E
F

Figure 17

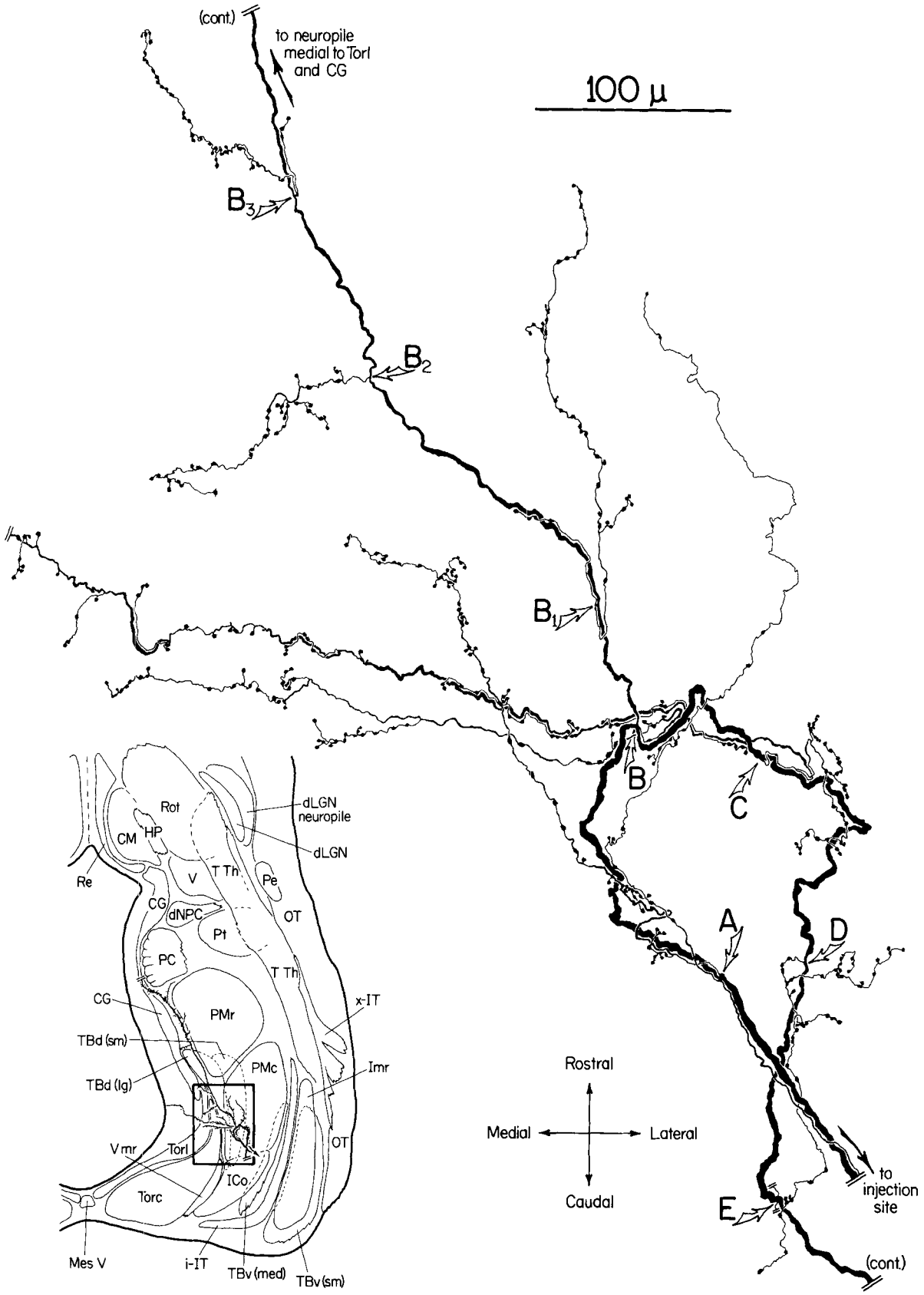

Fig. 18. High-magnification view of region B of the intermediate pathway axon illustrated in Figure 17. The medium caliber myelinated main trunk (2.5 μm diameter) begins giving off collaterals (lettered sequentially) immediately after leaving the tectum. Collaterals A–C support terminals in parts of profundus mesencephali caudalis (PMc), the intercollicular nucleus (ICo), and the central gray (CG). Collateral B is the "main rostral branch." It is by far the thickest collateral, approaching the diameter of the caudal trunk, and the only one that is consistently myelinated. The secondary collaterals emitted by collateral B are identified with subscripts. Most of the unmyelinated preterminal strands emitted from the rostral and caudal trunks remain close to the parent axon or travel medially, supporting small clusters of boutons scattered throughout a large volume. The inset shows one of the five sections used in this portion of the reconstruction. The rostral trunk is continued in Figures 19–21, while the caudal trunk is continued in Figures 22–25.

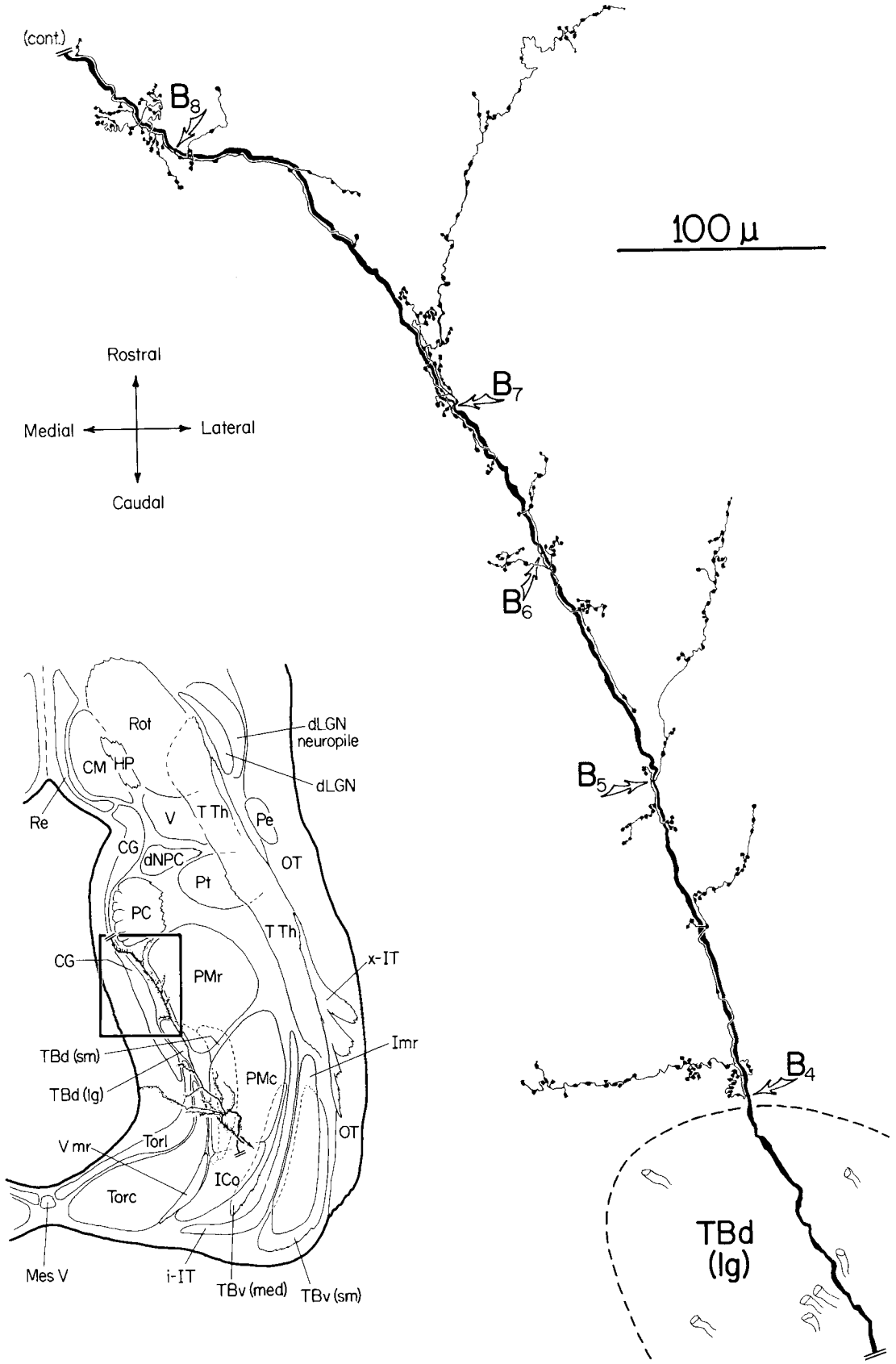

Fig. 19. High-magnification view of region A of the intermediate pathway axon illustrated in Figure 17. The myelinated main rostral branch begins emitting collaterals again (at B_4) immediately after passing through the bundle of large caliber dorsal pathway axons (TBd). These preterminal branches distribute small clumps of boutons to the neuropile between the central gray (CG) and profundus mesencephali rostralis (PMr). The main rostral collaterals of this and other TBi axons always avoided entering PMr. The inset shows one of the four sections used in this portion of the reconstruction.

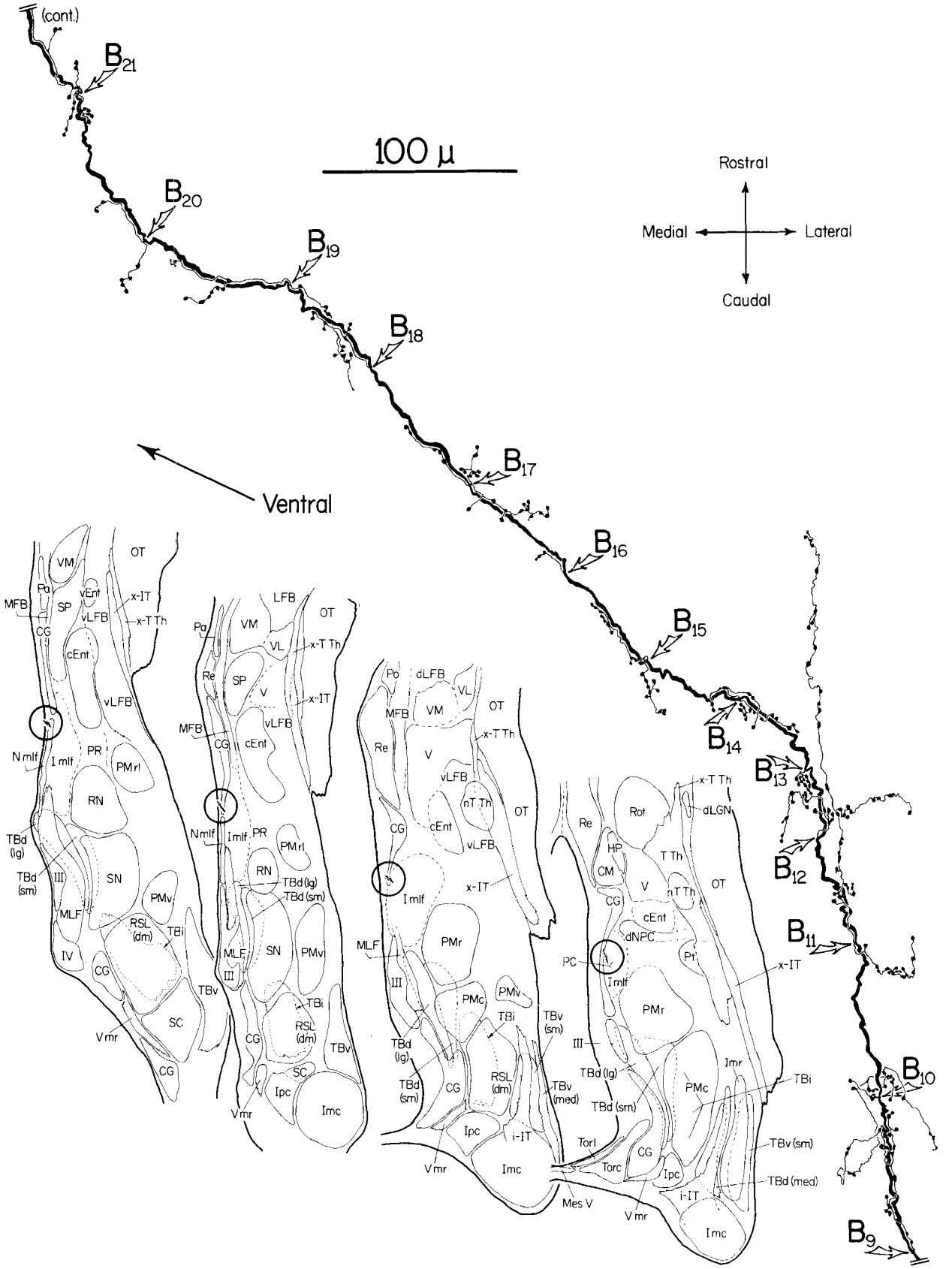

Fig. 20. High-magnification view of a portion of the intermediate pathway axon illustrated in Figure 17 that is just rostral to region A. The myelinated main rostral branch penetrates the central gray to run rostroventrally in the neuropile adjacent to the ependyma, where it emits a series of short collaterals. Ventrally, it reaches the rostral tip of the nucleus of the medial longitudinal fasciculus (Nmlf). The inset shows four of the eight sections used in this portion of the reconstruction.

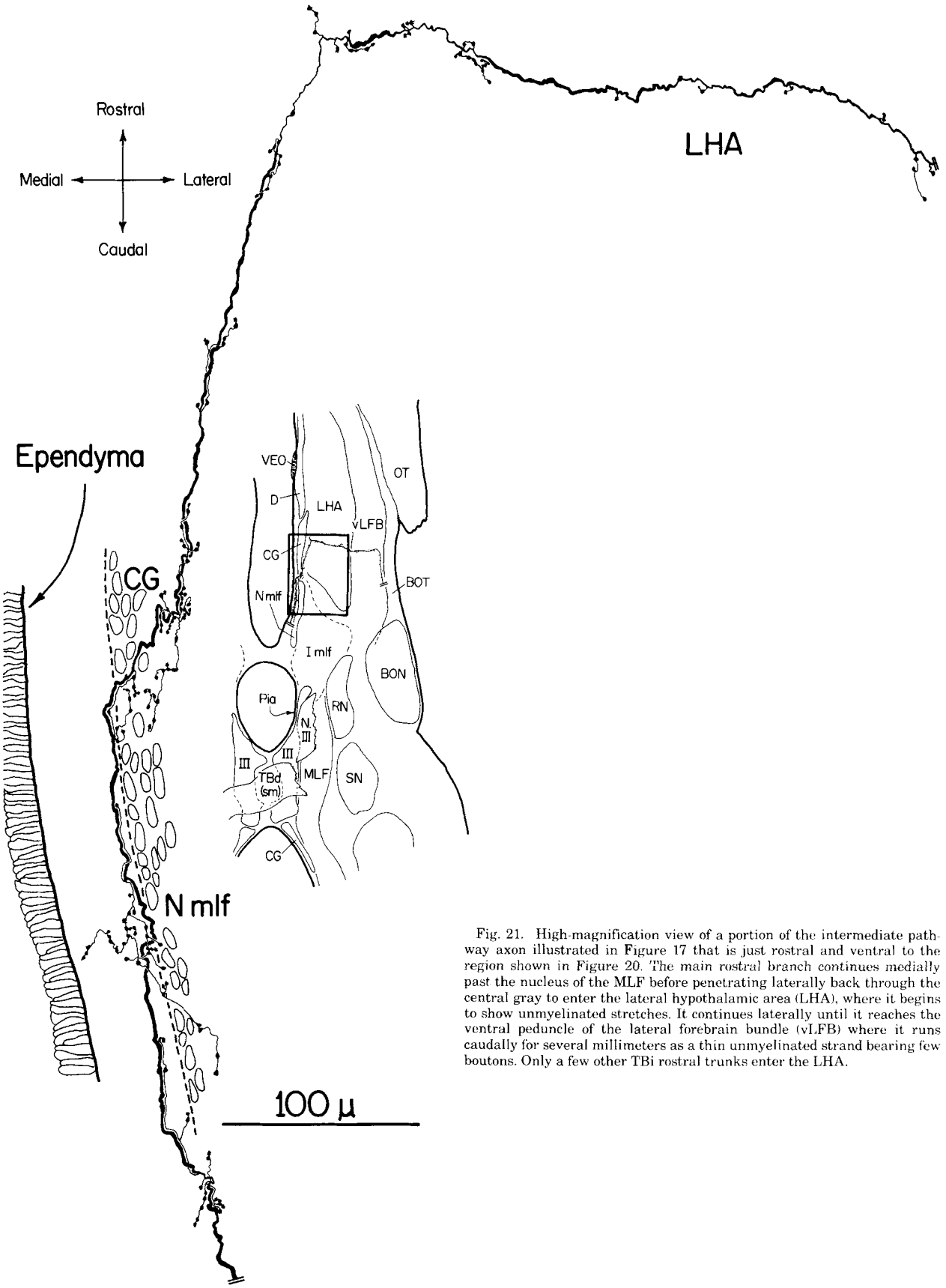

Fig. 21. High-magnification view of a portion of the intermediate pathway axon illustrated in Figure 17 that is just rostral and ventral to the region shown in Figure 20. The main rostral branch continues medially past the nucleus of the MLF before penetrating laterally back through the central gray to enter the lateral hypothalamic area (LHA), where it begins to show unmyelinated stretches. It continues laterally until it reaches the ventral peduncle of the lateral forebrain bundle (vLFB) where it runs caudally for several millimeters as a thin unmyelinated strand bearing few boutons. Only a few other TBi rostral trunks enter the LHA.

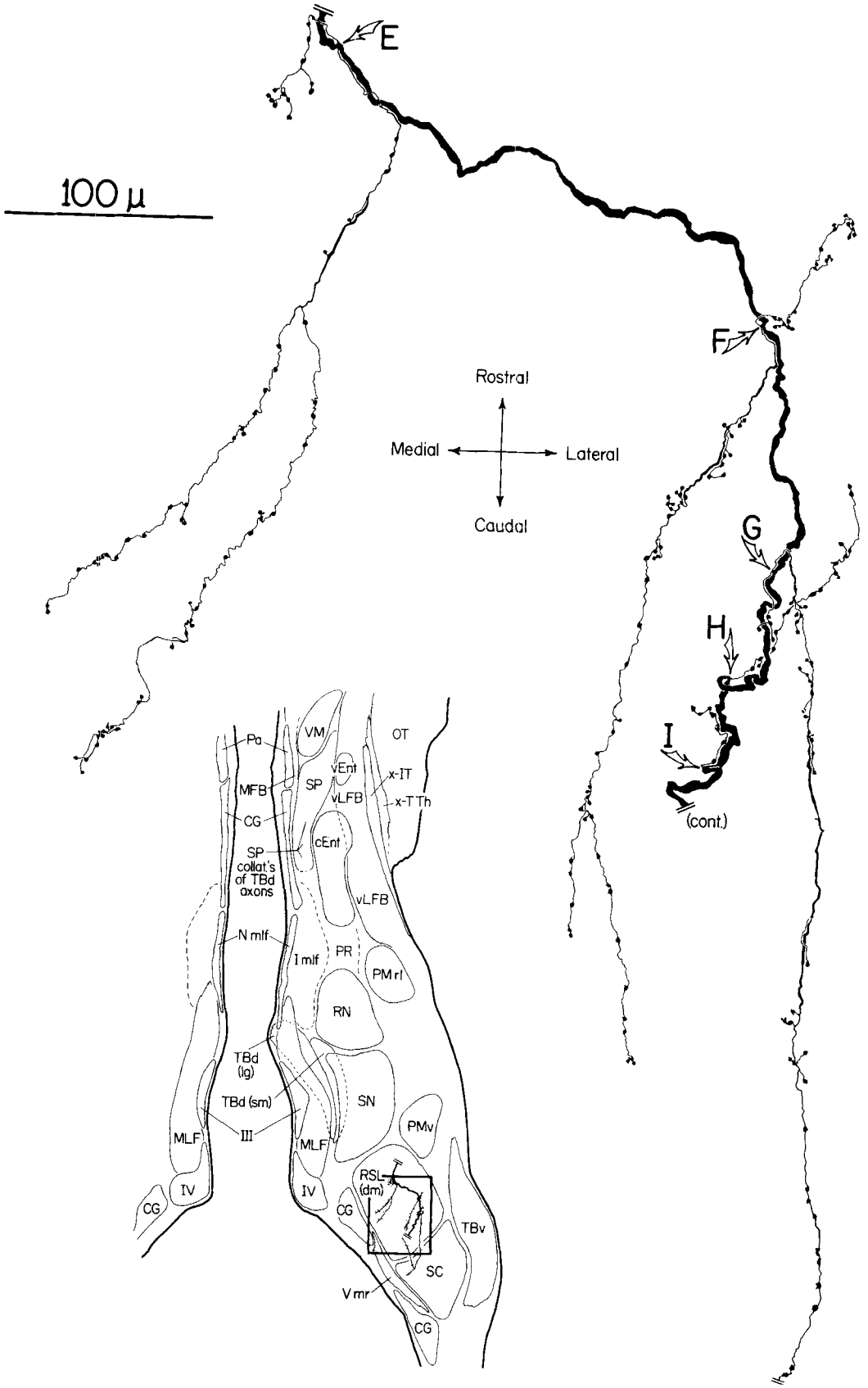

Fig. 22. High-magnification view of region C of the intermediate pathway axon illustrated in Figure 17. The main caudal trunk enters the dorsomedial segment of reticularis superioris lateralis (RSL(dm)), where it emits mostly medially or caudally directed preterminal strands at regular intervals bearing small clumps of medium-sized boutons. The main trunk turns ventrally (into the page) past collateral F and thus appears foreshortened until collateral I. RSL(dm) contains no magnocellular elements at this level. The inset shows one of the sections used in this portion of the reconstruction. Collateral G enters the small-celled nucleus (SC) ventral to the caudal magnocellular nucelus isthmi (Imc, not in section) and gives off a fine preterminal branch (see inset) bearing very small boutons.

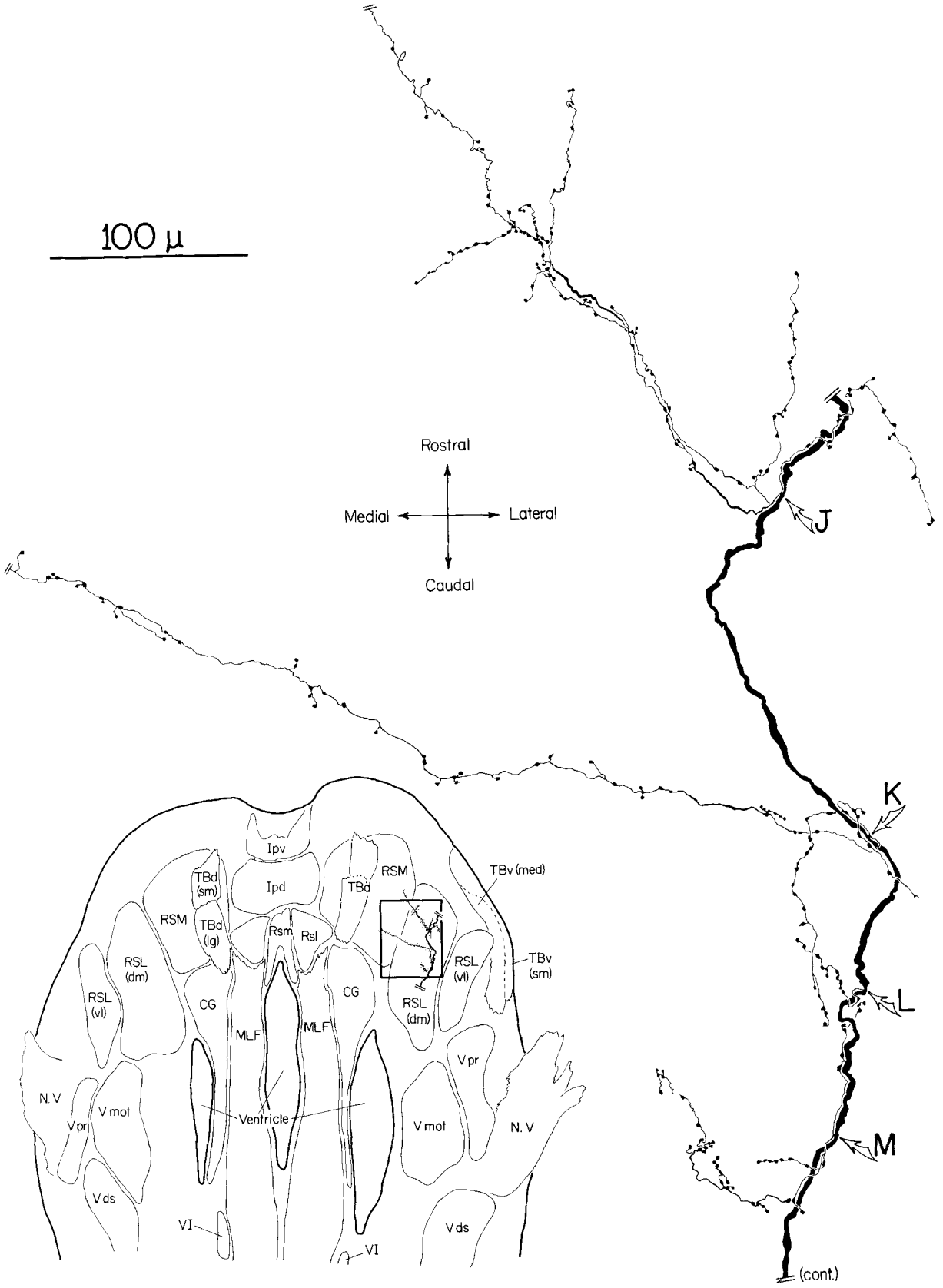

Fig. 23. High-magnification view of region D of the intermediate pathway axon illustrated in Figure 17. The main caudal trunk continues through the dorsomedial segment of reticularis superioris lateralis (RSL(dm)) emitting medially directed collaterals that sometimes penetrate the dorsal pathway terminal field in reticularis superioris medialis (RSM) (e.g., collaterals J and K). Conspicuous large cells appear in RSL(dm) at this level. The main trunk begins to recurve medially with other lateral brainstem structures after passing the bulge in the midline nuclei. The inset shows one of the sections used in this portion of the reconstruction.

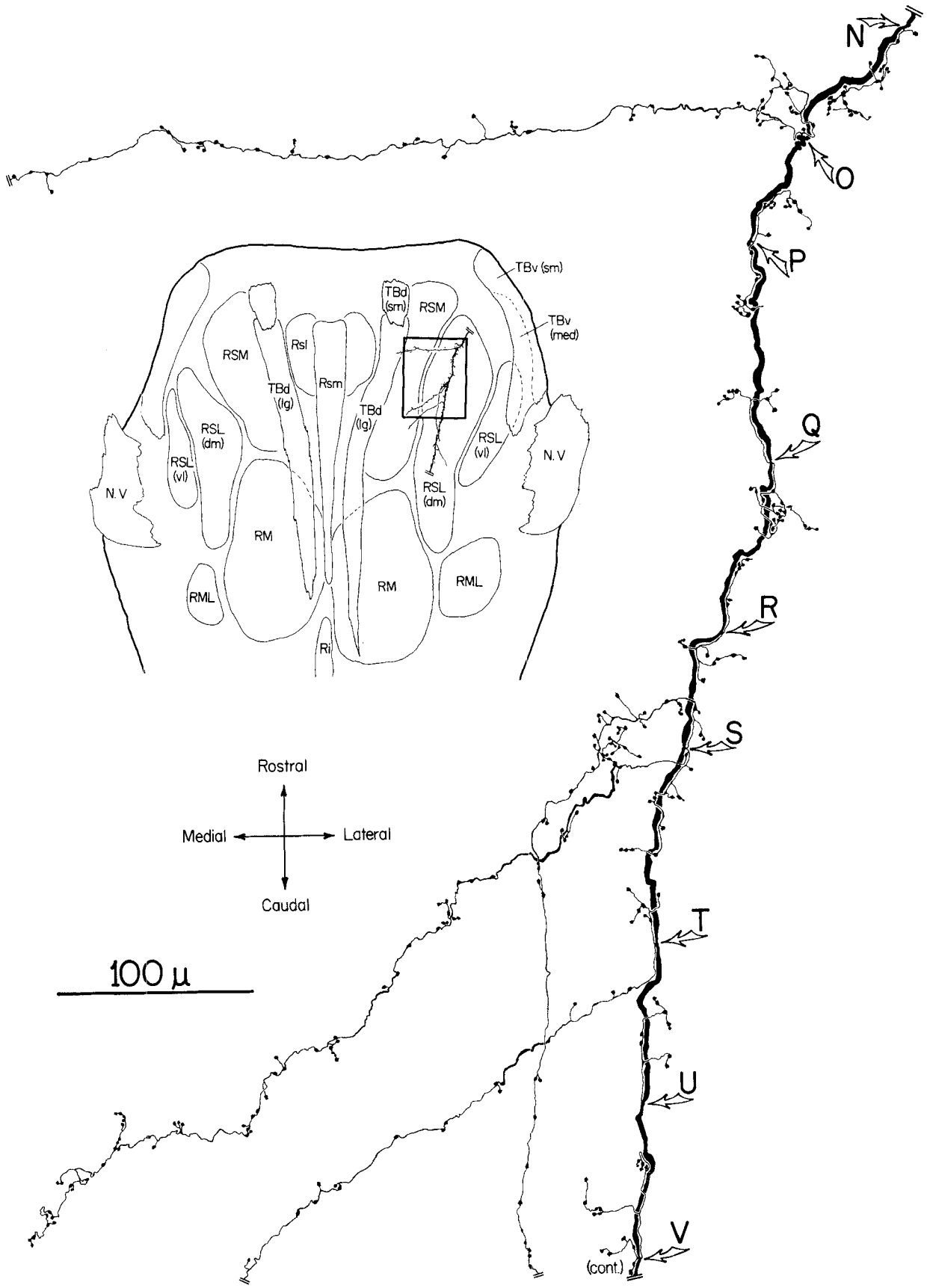

Fig. 24. High-magnification view of region E of the intermediate pathway axon illustrated in Figure 17. The main caudal trunk continues through the dorsomedial segment of reticularis lateralis (RSL(dm)), which still contains prominent magnocellular elements at this level. Several of the medially directed collaterals penetrate reticularis superioris medialis (RSM) but as before, most of the boutons are located in the lateral half of the reticular formation. The inset shows the location of this portion of the axon.

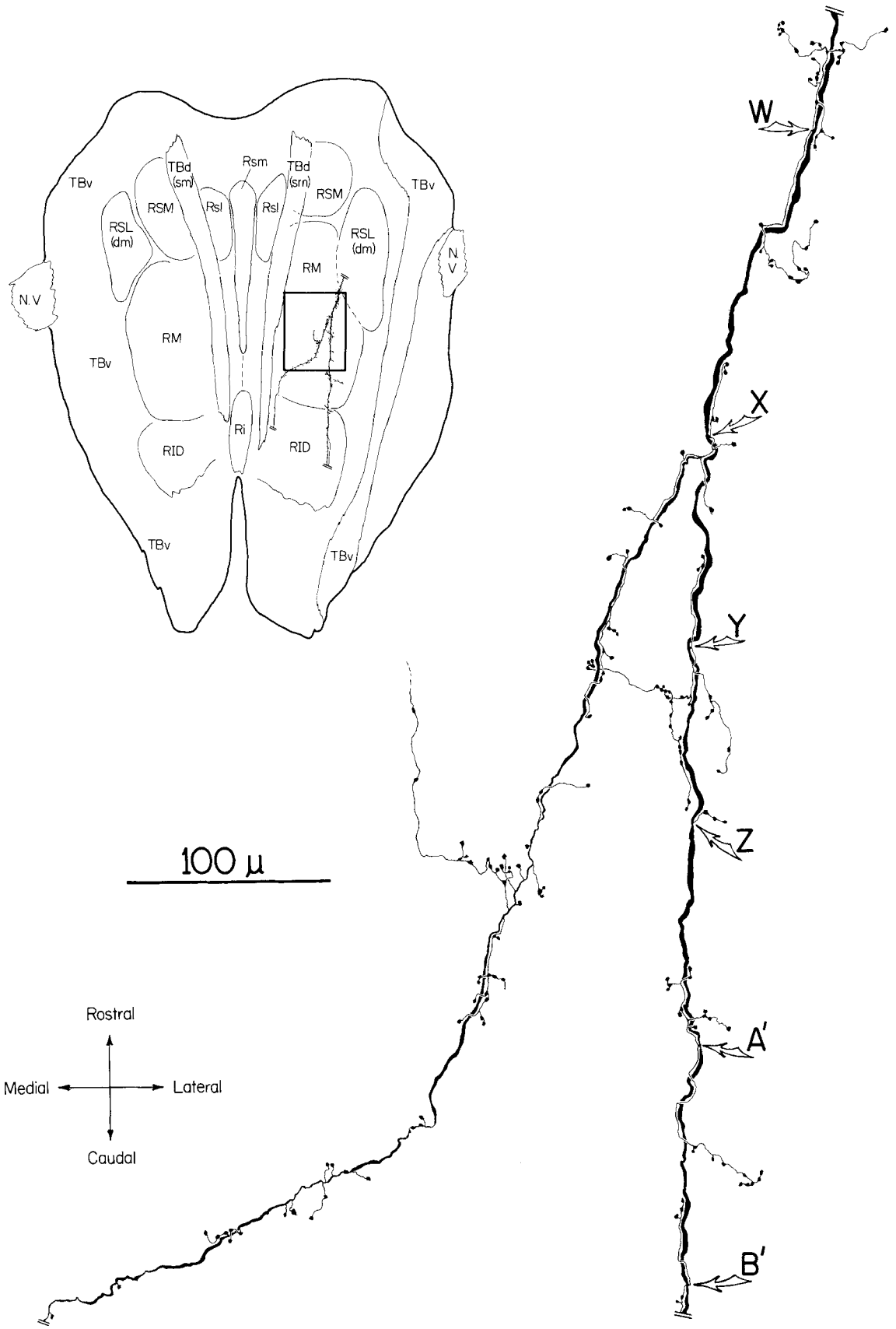

Fig. 25. High-magnification view of region F of the intermediate pathway axon illustrated in Figure 17. The main caudal trunk enters the medial half of reticularis medius (RM) where it emits a particularly thick medially directed collateral that almost reaches the midline, but supports few boutons in the medial parts of RM. The main trunk begins to thin as it continues caudally, emitting collaterals at regular intervals. It eventually enters the lateral parts of reticularis inferioris dorsalis (RID, see inset). HRP filling was less dense caudal to the portion of the reconstruction shown in the inset. As before, most of the boutons are located lateral to the TBd terminal field.

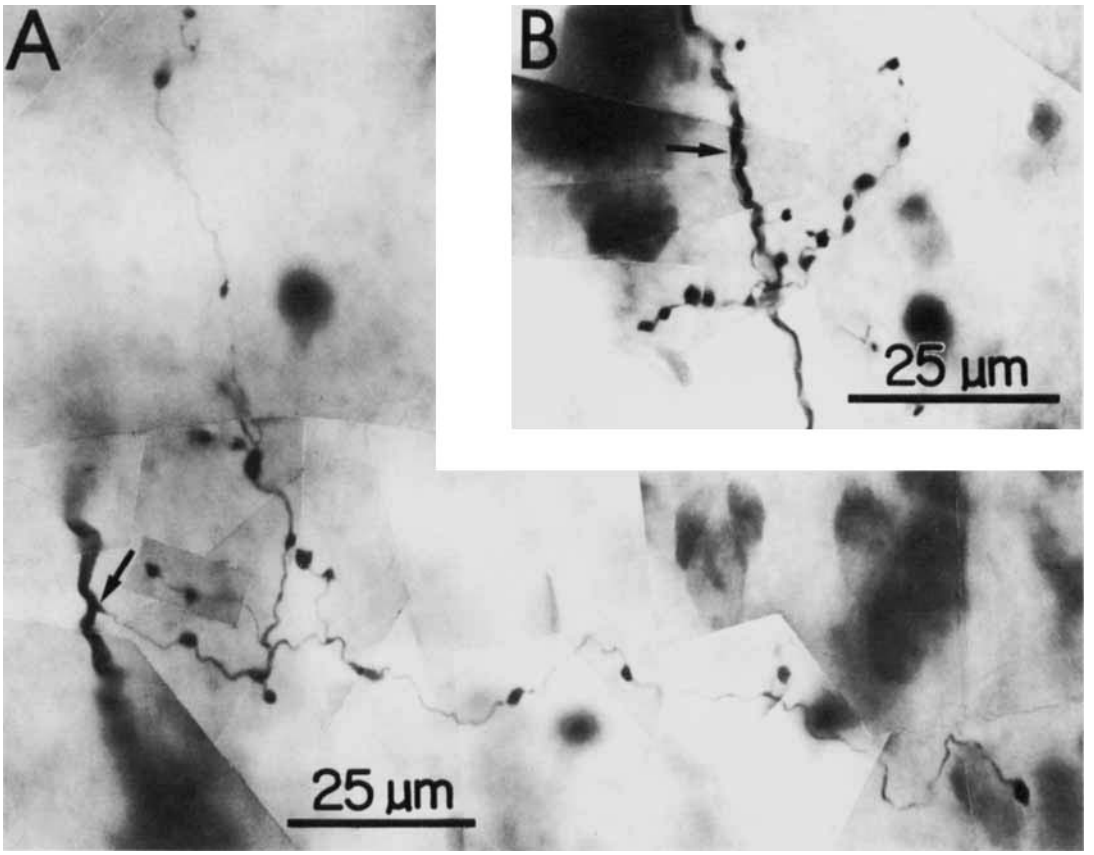

Fig. 26. Photomontage of tectoreticular axon collaterals. A shows a TBi collateral that arborized in the smaller-celled portion of the dorsomedial segment of reticularis superioris lateralis (RSL(dm)). B shows a TBd collateral that arose ipsilaterally in PMr (at asterisk in Fig. 7). The arrows indicate the origin of these thin preterminal branches. The parent trunks were apparently myelinated.

Fig. 27. Reconstruction of the intratectal collaterals of an axon arising from a cell in the stratum fibrosum et griseum superficiale (SFGS) and entering the small caliber component of the ventral pathway, TBv(sm). This cell was labeled by a lateral tegmental injection (see Sereno and Ulinski, '85). Immediately after its origin from the descending dendrite of the cell, the axon begins to emit collaterals downward into the stratum griseum centrale (SGC) and the stratum album centrale (SAC), at 100–200 μm intervals. Some branches reach the stratum griseum periventriculare (SGP). Further caudally, the axon emits collaterals into the small-celled nucleus (SC) and then in the ventrolateral tegmental neuropile (see schematic diagram) after passing through rostral magnocellular isthmi (Imr) without branching.

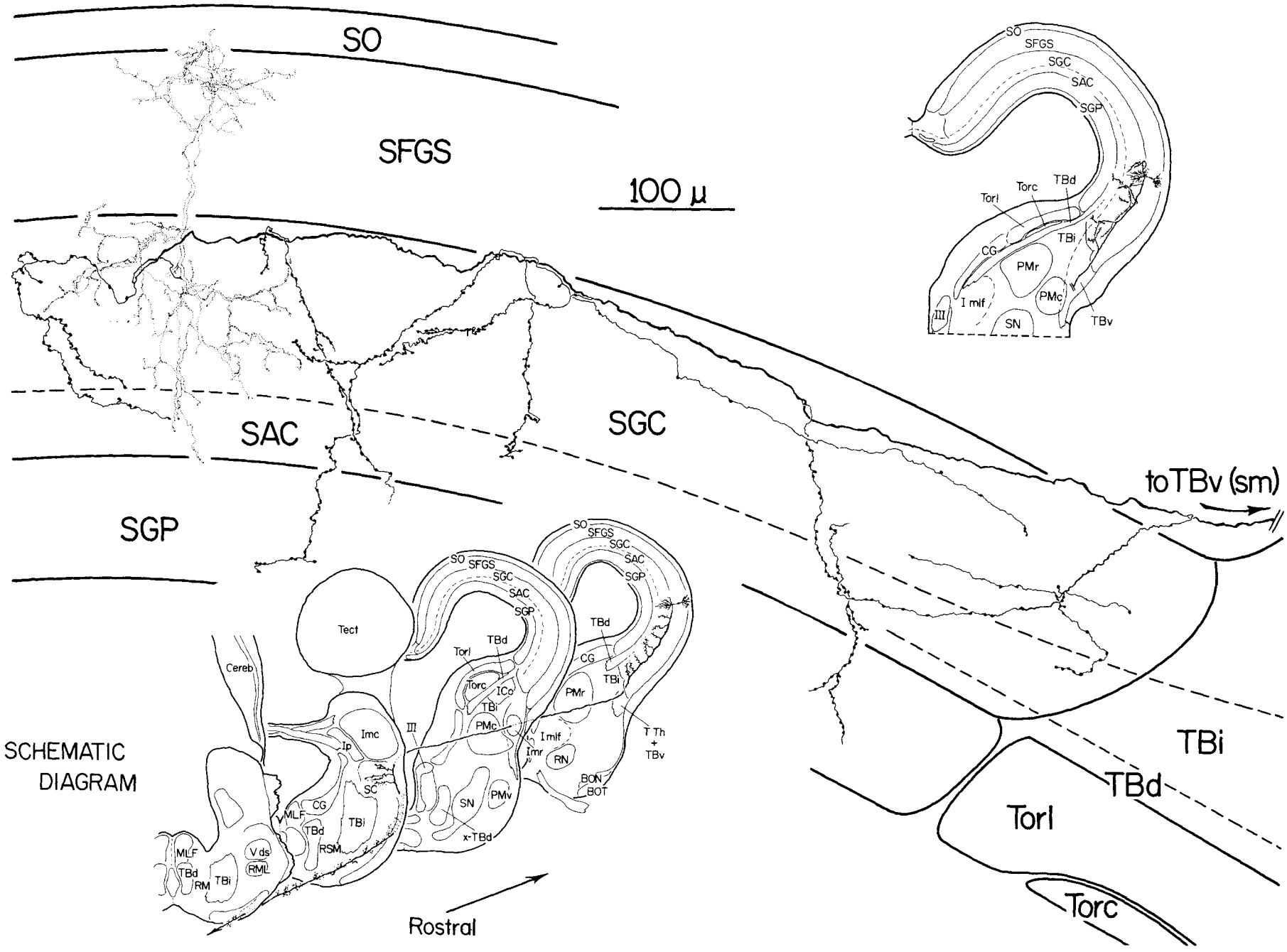
SO
SFGS
SAC
SGP
100 μ
SGC
toTBv (sm)
TBi
TBd
Torl
Torc
SCHEMATIC
DIAGRAM
Rostral
Tect
Cereb
Imc
Ip
SC
CG
MLF
TBd
TBi
RSM
V ds
RML
RM
III
ICo
PMc
PMr
I mlf
Imr
RN
SN
PMv
x-TBd
BON
BOT
T Th
+
TBv

Figure 27

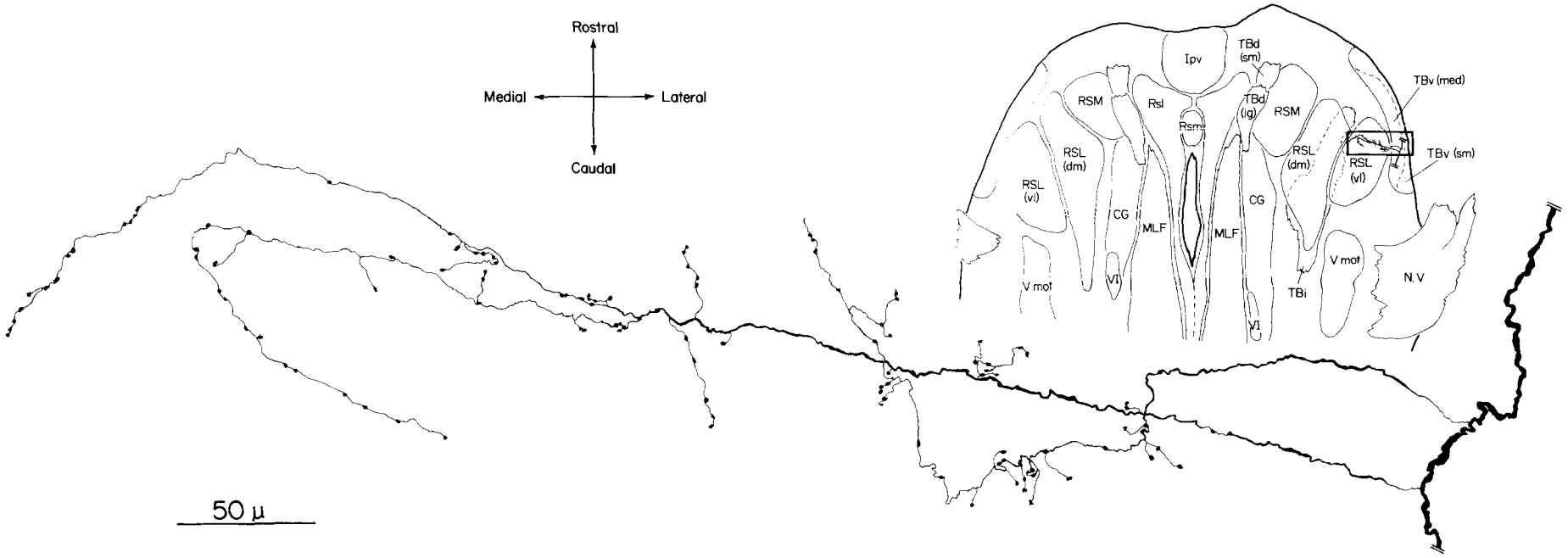

Fig. 28. Reconstruction from horizontal sections of two collaterals arising from an axon in the medium caliber component of the ventral pathway, TBv(med). These branches were confined to the ventrolateral segment of reticularis superioris lateralis (RSL(vl)). The main trunk of this axon was traced toward the tectal injection site through ten 110 μm serial sections but showed no additional branches before it was lost near rostral magnocellular isthmi (Imr). Caudally, several more widely spaced branches arose. Typically, TBv(med) axons do not branch as regularly as do TBi and TBd axons.

Fig. 29. Stereoscopic view of the main trunks of 17 intermediate pathway (TBi) axons emerging from two punctate injection sites and coursing into the lateral pontine reticular formation. Two small HRP injections at A and B (insets) labeled eight (Nos. 1–8) and nine (Nos. 9–17) TBi axons, respectively. These axons were traced through sixteen 110 μm serial horizontal sections into the dorsomedial segment of reticularis superioris lateralis (RSL(dm)), where they formed two spatially discrete clumps, each, however, containing a mixture of axons from the two injection sites. The more ventral clump, for instance, consists of axons numbers 2, 3, 6, and 8 (site A) and numbers 9, 14, and 15 (site B). The axons emerging from site A are drawn thicker only to make it easier to distinguish them from site B axons; all axons in fact were of similar caliber (1.5–2.5 μm). The stereodiagram can be viewed by ocular deviation or by using a standard stereoviewer. Axon number 2 (circled) is the axon reconstructed in detail in Figures 17–25.

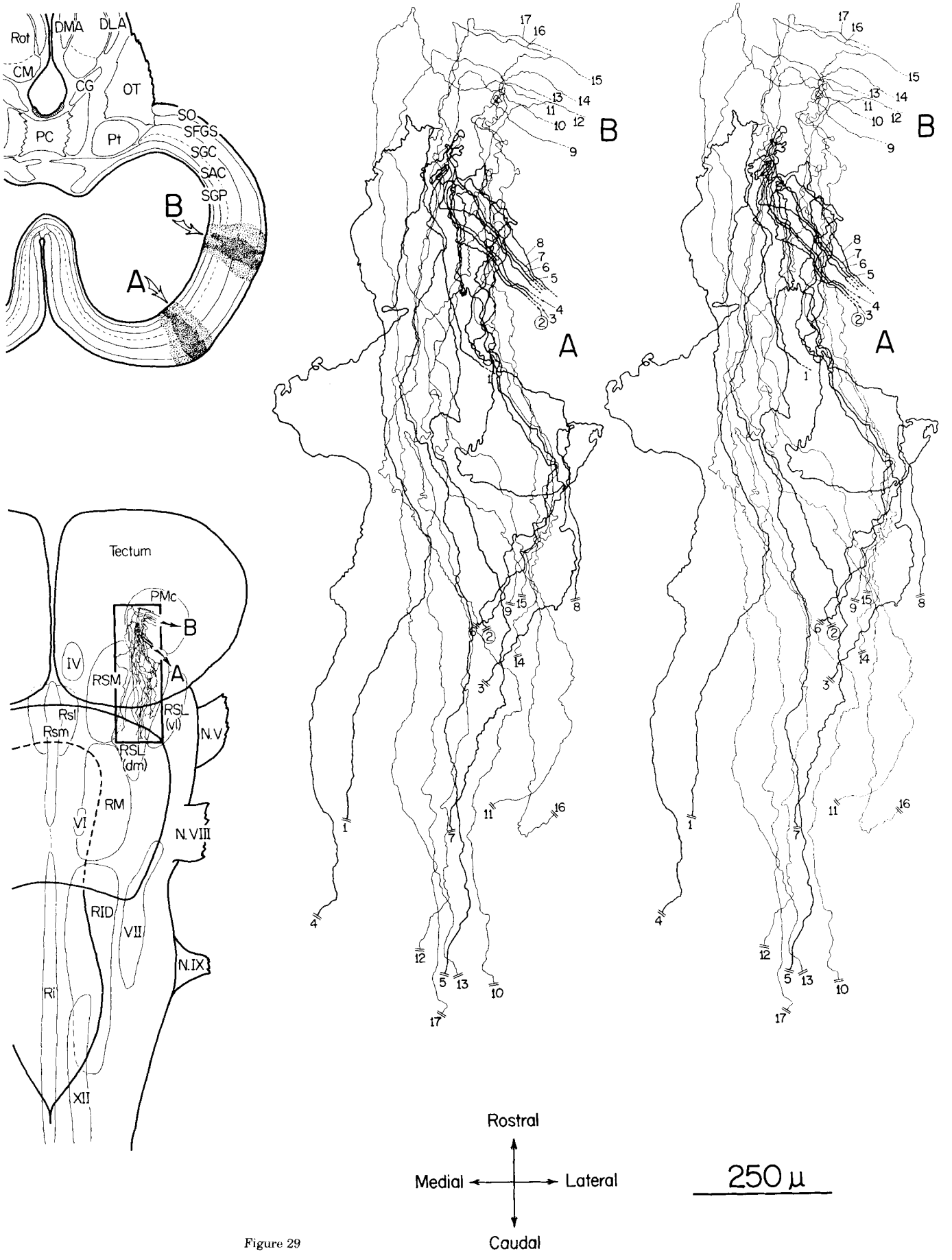
Rot
DMA
DLA
CM
CG
OT
PC
Pt
SO
SFGS
SGC
SAC
SGP
B
A
Tectum
PMc
IV
RSM
RSL (vl)
RSL (dm)
Rsl
Rsm
N.V
RM
VI
N.VIII
RID
VII
N.IX
Ri
XII
Rostral
Medial
Lateral
Caudal
250 μ

Figure 29

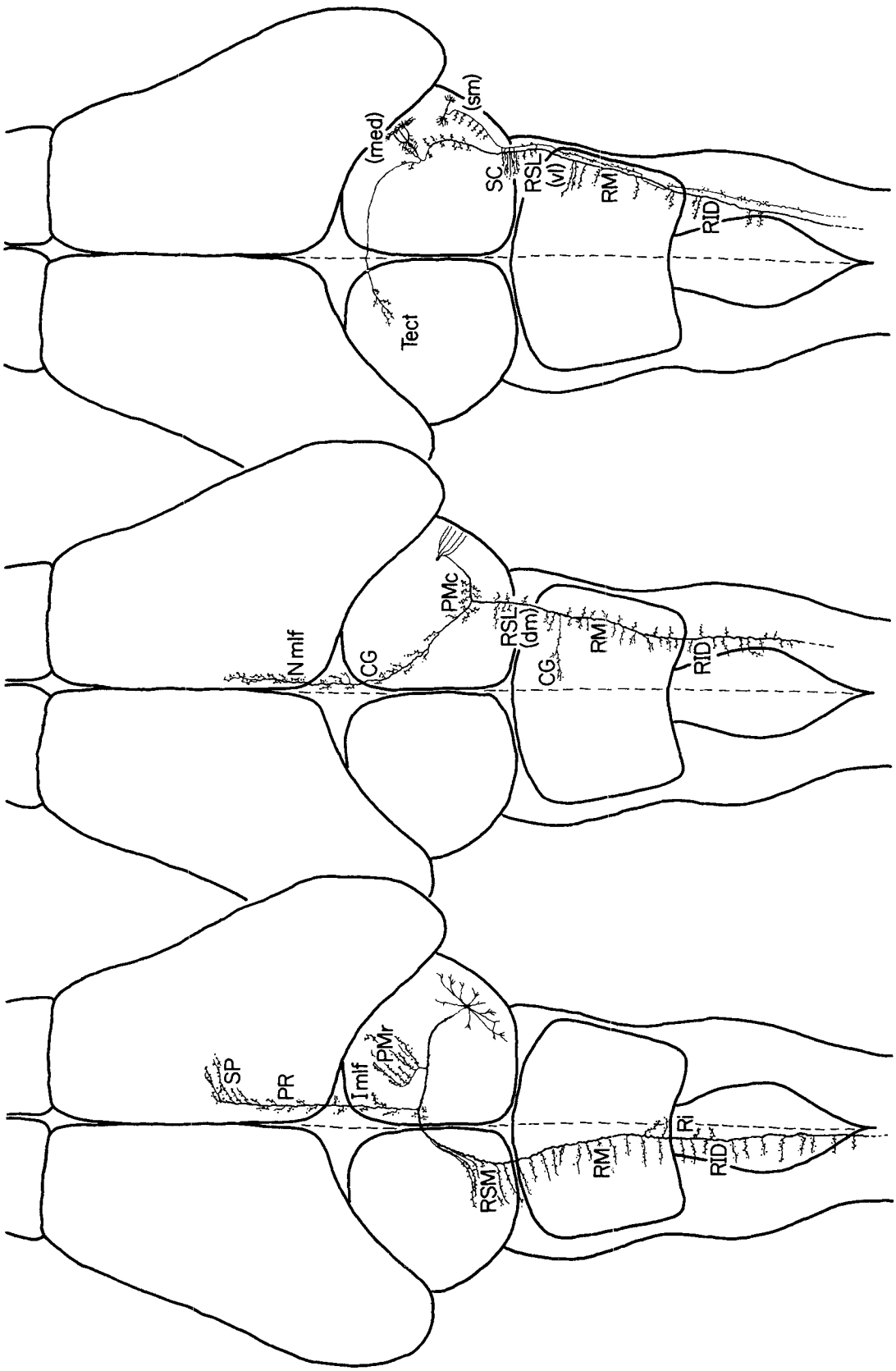

Fig. 30. Schematic diagram of typical branching patterns for single tectobulbar axons in each of the pathways. The dendritic morphologies are taken from Sereno and Ulinski ('85) and are drawn approximately to scale.

Bangma, G.C., and H.J. ten Donkelaar (1982) Afferent connections of the cerebellum in various types of reptiles. J. Comp. Neurol. *207*:255–273.

Bass, A.H. (1977) Effects of lesions of the optic tectum on the abilities of turtles to locate food stimuli. Brain Behav. Evol. *14*:251–260.

Bass, A.H., and R.G. Northcutt (1981) Retinal recipient nuclei in the painted turtle, *Chrysemys picta*: An autoradiographic and HRP study. J. Comp. Neurol. *199*:97–112.

Bass, A.H., M.B. Pritz, and R.G. Northcutt (1973) Effects of telencephalic and tectal ablations on visual behavior in the side-necked turtle, *Podocnemius unifilis*. Brain Res. *55*:455–460.

Bastian, J. (1982) Vision and electroreception: Integration of sensory information in the optic tectum of the weakly electric fish *Apteronotus albifrons*. J. Comp. Phsyiol. *147*:287–297.

Belekhova, M.G. (1979) Neurophysiology of the forebrain. In C. Gans, R.G. Northcutt, and P. Ulinski (eds): Biology of the Reptilia, Vol. 10, Neurology B. London: Academic, pp. 247–359.

Brauth, S.E., A. Reiner, C.A. Kitt, and H.J. Karten (1983) The substance P-containing striatotegmental path in reptiles: An immunohistochemical study. J. Comp. Neurol. *219*:305–327.

Brown-Gould, B. (1980) Organization of Afferents from the Brain Stem Nuclei to the Cerebellar Cortex in the Cat. Adv. Anat. Embryol. Cell Biol., Vol. 62. New York: Springer-Verlag.

Burne, R.A., S.A. Azizi, G.A. Milhailoff, and D.J. Woodward (1981) The tectopontine projection in the rat with comments on the visual pathways to basilar pons. J. Comp. Neurol. *202*:287–307.

Buttner-Ennever, J.A., and U. Buttner (1978) A cell group associated with vertical eye movements in the rostral mesencephalic reticular formation of the monkey. Brain Res. *151*:31–47.

Clarke, P.G.H. (1977) Some visual and other connections to the cerebellum of the pigeon. J. Comp. Neurol. *174*:535–552.

Cruce, W.L.R., and R. Nieuwenhuys (1974) The cell masses in the brain stem of the turtle *Testudo hermanni*: A topographical and topological analysis. J. Comp. Neurol. *156*:277–306.

Dacey, D.M. (1982) Neural Organization of the Optic Tectum in the Eastern Garter Snake, *Thamnophis sirtalis*: Structural Analysis of a Sensorimotor Transformation. Ph.D. dissertation, University of Chicago.

Ebbesson, S.O.E., and H. Vanegas (1976) Projections of the optic tectum in two teleost species. J. Comp. Neurol. *165*:161–180.

Ewert, J.-P. (1970) Neural mechanisms of prey-catching and avoidance behavior in the toad (*Bufo bufo L.*). Brain Behav. Evol. *3*:36–56.

Ferrier, D. (1886) The Functions of the Brain. New York: Smith, Elder, and Co.

Foster, R.E., and W.C. Hall (1975) The connections and laminar organization of the optic tectum in a reptile (*Iguana iguana*). J. Comp. Neurol. *163*:397–426.

Glenn, L.L., and R.E. Burke (1981) A simple and inexpensive method for 3-dimensional visualization of neurons reconstructed from serial sections. J. Neurosci. Methods *4*:127–134.

Graham, J., H.E. Pearson, N. Berman, and E.H. Murphy (1981) Laminar organization of superior colliculus in the rabbit: A study of receptive field properties of single units. J. Neurophysiol. *45*:915–932.

Grantyn, A.A., and A. Berthoz (1977) Synaptic actions of the superior colliculus on medial rectus motoneurons in the cat. Neuroscience *2*:945–951.

Grantyn, A., and R. Grantyn (1976) Synaptic actions of tectofugal pathways on abducens motoneurons in the cat. Brain Res. *105*:269–285.

Grantyn, A., and R. Grantyn (1982) Axonal patterns and sites of termination of cat superior colliculus neurons projecting in the tecto-bulbospinal tract. Exp. Brain Res. *46*:243–256.

Grantyn, A., R. Grantyn, and A. Berthoz (1982) Tectal control of vertical eye movements: A search for the underlying circuits in the mesencephalon. In A. Roucoux and M. Crommelinck (eds): Physiological and Pathological Aspects of Eye Movements. The Hague: Dr. W. Junk Publishers, pp. 337–344.

Grobstein, P., C. Comer, and S.K. Kostyk (1983) Frog prey capture behavior: between sensory maps and directed motor output. In J.-P. Ewert, R.R. Capranica, and D.J. Ingle (eds): Advances in Vertebrate Neuroethology. New York: Plenum, pp. 331–347.

Guitton, D., M. Crommelinck, and A. Roucoux (1980) Stimulation of the superior colliculus in the alert cat. I. Eye movements and neck EMG activity when head is restrained. Exp. Brain Res. *39*:63–73.

Harting, J.K. (1977) Descending pathways from the superior colliculus: An autoradiographic analysis in the rhesus monkey (*Macaca mulatta*). J. Comp. Neurol. *173*:583–612.

Harting, J.K., M.F. Huerta, A.J. Frankfurter, N.L. Strominger, and G.J. Royce (1980) Ascending pathways from the monkey superior colliculus: An autoradiographic analysis. J. Comp. Neurol. *192*:852–882.

Hartline, P.H., L. Kass, and M.S. Loop (1978) Merging of modalities in the optic tectum: Infrared and visual integration in rattlesnakes. Science *199*:1225–1229.

Hartline, P.H. (1984) The optic tectum of reptiles: Neurophysiological studies. In H. Vanegas (ed): Comparative Neurology of the Optic Tectum. New York: Plenum, pp. 601–618.

Holcombe, V., and W.C. Hall (1981a) Laminar origin of ipsilateral tectopontine pathways. Neuroscience *6*:255–260.

Holcombe, V., and W.C. Hall (1981b) The laminar origin and distribution of the crossed tectoreticular pathways. J. Neurosci. *1*:1103–1112.

Huber, G.C., and E.C. Crosby (1933) The reptilian optic tectum. J. Comp. Neurol. *57*:57–164.

Huerta, M.F., and J.K. Harting (1982) Tectal control of spinal cord activity: Neuroanatomical demonstration of pathways connecting the superior colliculus with the cervical spinal cord grey. In H.G.J.M. Kuypers and G.F. Martin (eds): Descending Pathways to the Spinal Cord. Prog. Brain Res. *57*:293–328.

Hunt, S.P., and H. Künzle (1976) Observations on the projections and intrinsic organization of the pigeon optic tectum: An autoradiographic study based on anterograde and retrograde, axonal and dendritic flow. J. Comp. Neurol. *170*:153–172.

Ingle, D.J. (1982) Organization of visuomotor behaviors in vertebrates. In D.J. Ingle, M.A. Goodale, and R.J.W. Mansfield (eds): Analysis of Visual Behavior. Cambridge: M.I.T. Press, pp. 67–109.

Jay, M.F., and D.L. Sparks (1982) Auditory and saccade-related activity in the superior colliculus of the monkey. Soc. Neurosci. Abstr. *8*:951.

Kawamura, K., A. Brodal, and G. Hoddevik (1974) The projection of the superior colliculus onto the reticular formation of the brainstem: An experimental anatomical study in the cat. Exp. Brain Res. *19*:1–19.

Künzle, H., and W. Woodson (1982) Mesodiencephalic and other target regions of ascending spinal projections in the turtle, *Pseudemys scripta elegans*. J. Comp. Neurol. *212*:349–364.

Luiten, P.G.M. (1981) Afferent and efferent connections of the optic tectum in the carp (*Cryprinus carpio* L.). Brain Res. *220*:51–65.

McIlwain, J.T. (1975) Visual receptive fields and their images in superior colliculus of the cat. J. Neurophysiol. *38*:219–230.

Maeda, M., T. Shibazaki, and K. Yoshida (1979) Labyrinthine and visual inputs to superior colliculus neurons. In R. Granit and O. Pompeiano (eds). Prog. Brain Res. *50*:735–743.

Mrosovsky, N., A.M. Granda, and T. Hay (1979) Seaward orientation of hatchling turtles: Turning systems in the optic tectum. Brain Behav. Evol. *16*:203–221.

Nagata, T. and L. Kruger (1979) Tactile neurons of the superior colliculus of the cat: Input and physiological properties. Brain Res. *174*:19–37.

Newman, D.B., W.L.R. Cruce, and L.L. Bruce (1983) The sources of supraspinal afferents to the spinal cord in a variety of limbed reptiles. I. Reticulospinal systems. J. Comp. Neurol. *215*:17–32.

Palmer, A.R., and A.J. King (1982) The representation of auditory space in the mammalian superior colliculus. Nature *299*:248–249.

Papez, J.W. (1935) Thalamus of turtles and thalamic evolution. J. Comp. Neurol. *61*:433–475.

Parent, A. (1979) Monoaminergic systems of the brain. In C. Gans, R.G. Northcutt, and P. Ulinski (eds) : Biology of the Reptilia, Vol. 10, Neurology B. London: Academic, pp. 247–285.

Rainey, W.T. (1978) Organization of nucleus rotundus, a tectofugal thalamic nucleus in turtles. I. Nissl and Golgi analysis. J. Comp. Neurol. *160*:121–142.

Ramón, P. (1896) Estructura de encefalo del camaleon. Rev. Trim. Micrograf. *1*:146–182.

Roucoux, A., D. Guitton, and M. Crommelinck (1980) Stimulation of the superior colliculus in the alert cat. II. Eye and head movements evoked when the head is unrestrained. Exp. Brain Res. *39*:75–85.

Rubinson, K. (1968) Projections of the optic tectum of the frog. Brain Behav. Evol. *1*:529–561.

Schnyder, H., and H. Künzle (1983) The retinopetal system in the turtle *Pseudemys scripta elegans*. Cell Tissue Res. *234*:219–224.

Sereno, M.I. (1983) Dendritic and axonal morphology of tectal-projecting neurons in the isthmus region of a turtle, *Pseudemys scripta*. Proc. Soc. Neurosci. *9*:818 (Abstract).

Sereno, M.I., and P.S. Ulinski (1985) Tectoreticular pathways in the turtle

Pseudemys scripta. II. Morphology of tectoreticular cells. J. Comp. Neurol. *233*:91–114.

Smeets, W.J.A.J. (1981) Efferent tectal pathways in two chondrichthyans, the shark *Scyliorhinus canicula* and the ray *Raja clavata*. J. Comp. Neurol. *195*:13–23.

Sparks, D.L., and L.E. Mays (1981) The role of the monkey superior colliculus in the control of saccadic eye movements: A current perspective. In A.F. Fuchs and W. Becker (eds): Progress in Oculomotor Research. New York: Elsevier, pp. 137–144.

Stein, B.E., and H.P. Clamann (1981) Control of pinna movements and sensorimotor register in cat superior colliculus. Brain Behav. Evol. *19*:180–192.

Stein, B.E., and N.S. Gaither (1981) Sensory representation in reptilian optic tectum: Some comparisons with mammals. J. Comp. Neurol. *202*:60–87.

Stein, B.E., and N.S. Gaither (1983) Receptive-field properties in reptilian optic tectum: Some comparisons with mammals. J. Neurophysiol. *50*: 102–124.

ten Donkelaar, H.J., and R. Nieuwenhuys (1979) The brainstem. In C. Gans, R.G. Northcutt, and P. Ulinski (eds): Biology of the Reptilia, Vol. 10, Neurology B. London: Academic, pp. 133–200.

Ulinski, P.S. (1977) Tectal efferents in the banded water snake. J. Comp. Neurol. *173*:251–274.

Wang, R., J.L. Kubie, and M. Halpern (1977) Brevital Sodium: An effective anesthetic agent for performing surgery on small reptiles. Copeia *1977*:738–743.

Wurtz, R.H., and J.E. Albano (1980) Visual-motor functions of the primate superior colliculus. Annu. Rev. Neurosci. *3*:189–226.